June 1990

UILU-ENG-90-2220
DC-119

COORDINATED SCIENCE LABORATORY
College of Engineering
Decision and Control Laboratory

ADAPTIVE CONTROL OF AN ARC WELDING PROCESS

Daniel Edward Henderson

UNIVERSITY OF ILLINOIS AT URBANA-CHAMPAIGN

UNCLASSIFIED

SECURITY CLASSIFICATION OF THIS PAGE

REPORT DOCUMENTATION PAGE

Form Approved OMB No. 0704-0188

1a. REPORT SECURITY CLASSIFICATION Unclassified	1b. RESTRICTIVE MARKINGS None
2a. SECURITY CLASSIFICATION AUTHORITY	3. DISTRIBUTION/AVAILABILITY OF REPORT Approved for public release; distribution unlimited
2b. DECLASSIFICATION/DOWNGRADING SCHEDULE	
4. PERFORMING ORGANIZATION REPORT NUMBER(S) UILU-ENG-90-2220 DC-119	5. MONITORING ORGANIZATION REPORT NUMBER(S)
6a. NAME OF PERFORMING ORGANIZATION Coordinated Science Lab University of Illinois 6b. OFFICE SYMBOL (If applicable) N/A	7a. NAME OF MONITORING ORGANIZATION US Army Construction Research Laboratory
6c. ADDRESS (City, State, and ZIP Code) 1101 W. Springfield Ave. Urbana, IL 61801	7b. ADDRESS (City, State, and ZIP Code) P. O. Box 4005 Champaign, IL 61824-4005
8a. NAME OF FUNDING/SPONSORING ORGANIZATION US Army Construction Res. Lab 8b. OFFICE SYMBOL (If applicable)	9. PROCUREMENT INSTRUMENT IDENTIFICATION NUMBER DACA 88-90-D-0003-01
8c. ADDRESS (City, State, and ZIP Code) P. O. Box 4005 Champaign, IL 61824-4005	10. SOURCE OF FUNDING NUMBERS PROGRAM ELEMENT NO. / PROJECT NO. / TASK NO. / WORK UNIT ACCESSION NO.

11. TITLE (Include Security Classification)

ADAPTIVE CONTROL OF AN ARC WELDING PROCESS

12. PERSONAL AUTHOR(S)

HENDERSON, DANIEL EDWARD

13a. TYPE OF REPORT	13b. TIME COVERED	14. DATE OF REPORT (Year, Month, Day)	15. PAGE COUNT
Technical	FROM _____ TO _____	1990 June	62

16. SUPPLEMENTARY NOTATION

17. COSATI CODES			18. SUBJECT TERMS (Continue on reverse if necessary and identify by block number)
FIELD	GROUP	SUB-GROUP	Weld puddle, sensitivity points, off-line tuning, adaptive control.

19. ABSTRACT (Continue on reverse if necessary and identify by block number)

An adaptive system controlling weld puddle width is presented. It is based on the method of sensitivity points. The development of the general design is given. Simulated and experimental setup and results are presented.

20. DISTRIBUTION/AVAILABILITY OF ABSTRACT ☒ UNCLASSIFIED/UNLIMITED ☐ SAME AS RPT. ☐ DTIC USERS	21. ABSTRACT SECURITY CLASSIFICATION Unclassified
22a. NAME OF RESPONSIBLE INDIVIDUAL	22b. TELEPHONE (Include Area Code) / 22c. OFFICE SYMBOL

DD Form 1473, JUN 86 Previous editions are obsolete. SECURITY CLASSIFICATION OF THIS PAGE

UNCLASSIFIED

ADAPTIVE CONTROL OF AN ARC WELDING PROCESS

BY

DANIEL EDWARD HENDERSON

B.S., University of Illinois, 1989

THESIS

Submitted in partial fulfillment of the requirements
for the degree of Master of Science in Electrical Engineering
in the Graduate College of the
University of Illinois at Urbana-Champaign, 1990

Urbana, Illinois

ABSTRACT

An adaptive system controlling weld puddle width is presented. It is based on the method of sensitivity points. The development of the general design is given. Simulated and experimental setup and results are presented.

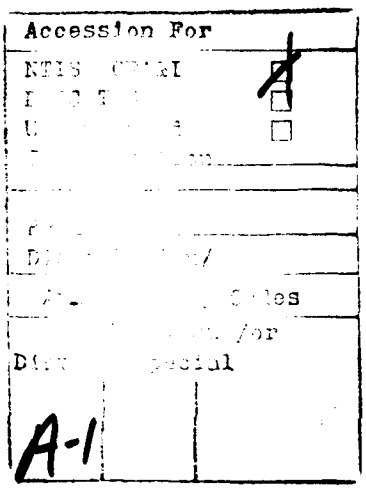

ACKNOWLEDGMENTS

I would like to thank my advisor, Professor P. V. Kokotović, for the encouragement and insight he has given me while under his tutelage. I would also like to thank Bob Weber and Frank Kearney for their support of this research. I would like to thank my research partners, Jeff Schiano and Jim Ross, for their ideas, their help, and the fun we have had while working on this project. I really want to thank my wife, Pam, for her patience, her support (in many ways), and for her partnership with me in this project. I would like to thank my parents, without whose help and support I would not have been able to pursue a college education. Most of all, I would like to thank Jesus Christ for the love, acceptance, and powerful support he has given me in my life.

TABLE OF CONTENTS

LIST OF TABLES

LIST OF FIGURES

CHAPTER 1

INTRODUCTION

The following research was conducted as part of a joint project for the University of Illinois Decision and Control Laboratory and the Metallurgy and Quality Assurance Team of the United States Army Construction Engineering Research Laboratory. The ultimate objective of the program is to develop an automated welding system which produces consistently good welds despite variations in material parameters and other disturbances. The scope of the research is limited to consumable-electrode gas metal arc welding (GMAW), since this is one of the most frequently employed and economically important welding processes.

It is well-known that the reliability of the weld is strongly correlated to the microstructure and overall geometry of the joint [1]. These properties are determined by the thermal and mechanical history of the weld puddle and the rate at which it cools. The thermomechanical dynamics are driven by the flow of heat and mass from the torch as it travels along the weld joint.

Since the shape of the molten weld puddle plays an important role in determining the integrity of the weld joint, several researchers have developed methods for measuring and regulating puddle geometry. Vroman and Brandt [2] measured puddle width using a line scan camera. By controlling torch velocity, they regulated puddle width using a PI

controller. Richardson [3]-[4] and Corby [5] designed an integrated through-torch vision system for coaxial puddle viewing. Baheti [6] developed an algorithm for estimating weld puddle area and width from coaxial images of the puddle. Baheti also designed a PID controller to regulate puddle width and area using arc current as the controlled variable. Suzuki and Hardt [7] proposed a model reference adaptive controller to regulate puddle width by adjusting arc current.

The goals of this research were to design, implement and experimentally evaluate a model reference adaptive puddle width control system which uses torch travel rate as the control input. The adaptation algorithm is based on the method of sensitivity points. The design and results of this work are presented here.

Chapter 2 describes the welding system and the image processing system used to measure puddle geometry and weld bead temperature information. It also describes the modeling of the system and the reference model used for this research. Chapter 3 gives the development of the sensitivity methods applicable to this type of system. It contains both off-line and on-line methods for automatic tuning. Chapter 4 reports the results of simulating the off-line automatic tuning methods as applied to the welding system models. Chapter 5 compares both the simulated and experimental results for the designed on-line adaptive system. Conclusions and recommendations are summarized in Chapter 6. The Appendix gives the experimental setup used.

CHAPTER 2

OVERALL SYSTEM DESCRIPTION

2.1 System Description

A dc power supply is connected between the workpiece and electrode contact tube. Consumable-electrode wire is fed to the workpiece through a set of pinch rollers. The wirefeed rate determines both the arc current and the rate of metal deposition. As the torch is moved along the workpiece, the joint is filled with a solution of electrode wire and workpiece material. The region surrounding the weld puddle is purged with a shield gas to prevent oxidation and contamination of the weld joint. In conventional GMAW, the controlled inputs are arc current and torch travel velocity. Other variables such as power supply voltage, shield gas flow rate, and the contact tube height are fixed prior to welding. The Appendix gives all of the values at which these variables were fixed for the experiments presented in this thesis.

The facility at which these GMAW control system experiments were performed was developed at the US Army Construction Engineering Research Laboratory in collaboration with the University of Illinois Decision and Control Laboratory. In this facility, a Sony CCD camera is attached to the torch for puddle viewing. Unlike a through-torch vision

system which views the puddle directly, the Sony camera is mounted behind the torch and views the puddle from an angle. This approach allows existing GMAW systems to be upgraded through the addition of such a camera and does not require replacement of the torch head. A drawback of this scheme is that the leading edge of the puddle is not visible. Puddle width and area are estimated using the algorithm developed by Baheti [6]. Since Baheti's algorithm requires information only at the trailing edge of the puddle, the lack of data from the leading edge is not a major disadvantage. A Compaq 386 33 MHz computer serves as a dedicated image processing system which can aquire an image and estimate the puddle geometry within 52 msec.

A second Compaq 386 33 MHz computer system implements control loops and supervises the image processing computer. A proportional plus sum (PI) controller is used in the servo loop to control the travel rate of the torch. The design of the wirefeed rate controller is complicated by torque disturbances imposed by the wire pinch rollers and wire spool. A polynomial design method was used to provide the desired closed-loop dynamics and disturbance rejection properties of the wirefeed rate servo loop [8]. The wirefeed servo loop is contained in the arc current servo loop. The arc current is controlled using a PI controller which generates the wirefeed command. The arc current controller gains were obtained using a linearized second-order model of the arc dynamics. These gains were fine-tuned using the method of Sensitivity Points [9]-[14].

Previous work has shown that the dominant time constant of the puddle width response is of the order of 2 sec [7]. Based on this expectation, the travel rate and arc current loops were designed with a response time of 0.2 sec which allows the dynamics of the travel rate and arc current control systems to be ignored when studying the puddle geometry response. The sample rate on the travel rate, wirefeed rate, and arc current control loops is 40 msec. The computational delay imposed by these three control loops is approximately

1 msec. The puddle width and area are measured every 400 msec using the image processing system.

2.2 Plant Modeling

Earlier work with this GMAW system has shown that the range of useful operation of the system extends with travel rate from 8 inches-per-minute (IPM) to 18 IPM and with arc current from 310 Amperes (A) to 410 A [11]. Based on this, Ross used recursive least-squares to identify three small-signal models of the travel rate reference input to puddle width output dynamics for a 1" thick plate pre-heated to a temperature of 250° F. He did this by stepping the travel rate by ± 2 IPM around the nominal travel rate of 13 IPM for three different arc currents, 310 A, 360 A, and 410 A [12]. The three resultant models are:
Nominal-Current (360 A) Model:

$$\frac{W(z)}{TR(z)} = \frac{-0.0006z^2 - 0.0032z - 0.0006}{z^4 - 1.0658z^3 + 0.01z^2 + 0.0383z + 0.1340} \tag{2.1}$$

High-Current (410 A) Model:

$$\frac{W(z)}{TR(z)} = \frac{0.0004z^2 - 0.0016z - 0.0023}{z^4 - 0.9716z^3 - 0.0427z^2 - 0.0543z + 0.1693} \tag{2.2}$$

Low-Current (310 A) Model:

$$\frac{W(z)}{TR(z)} = \frac{-0.0013z^2 + 0.0009z - 0.0039}{z^4 - 1.0377z^3 + 0.0641z^2 + 0.0682z + 0.037}. \tag{2.3}$$

These three plant models were used to describe the plant for the simulations done in this thesis. The nominal-current plant model is used in the pseudo-sensitivity model in the implementation of the on-line automatic tuning system presented in this thesis.

2.3 Reference Model

Preliminary work with the puddle width control system showed that the open-loop puddle width response to a travel rate step has a rise time of about 6 sec and overshoots by about 10%. This overshoot in puddle width leads to poor weld joints in the sense that the joint is not uniform and does not vary smoothly in response to steps in travel rate. Uniformity and smoothness of variations are desirable qualities of a weld joint because they are strongly related to the overall strength of the joint. Based on this information, a second-order puddle width reference model was designed with an overdamped step response and a rise time of about 10 sec. This corresponds to a $\zeta \simeq 1.1$ and $\omega_n \simeq 0.488$ [13]. The resulting reference model is

$$RM(z) = \frac{0.0165z + 0.0143}{z^2 - 1.62z + 0.6509}. \tag{2.4}$$

This model provides the desired response in the sensitivity point example in Chapter 3, and is used as the reference model in both the off-line and on-line automatic tuning systems presented in this thesis.

CHAPTER 3

SENSITIVITY METHODS

The use of sensitivity methods for the optimization of system parameters has been in practice for almost 30 years. Work done by Kokotović, Medanić, Perkins and others [14]-[20] in the early 1960s laid much of the foundation for the application of these methods to practical control problems. In particular, papers given by Kokotović, Hung, and Rhode [14, 18,21,22] present some simple, practical methods for the generation and use of sensitivity functions in the design of control systems. Results by Rhode using the method of averaging give stability proofs for the type of adaptive system designed here [18,22].

3.1 Sensitivity Function Concepts

The sensitivity method applied in this thesis is a simplified version of the form described in [14]. It is to be applied to the automatic tuning of a PI controller which controls weld puddle width using torch velocity as the control input. The PI controller was chosen for this system because of its robustness qualities and its simplicity, which make the implementation of this on-line automatic tuning system straightforward.

Consider a feedback system of the form shown in Figure 3.1. (The figures for each chapter are given at the end of the chapter.) Block C(K_p, K_i,z) represents a controller of known structure, and block G(z) represents the plant. The structure of the plant does not

have to be known.

For a given input, r(z), nominal parameters, K_p and K_i, and small parameter deviations, ΔK_p and ΔK_i, the output can be expressed as a Taylor expansion

$$\begin{aligned} w(K_p^0 + \Delta K_p, K_i^0 + \Delta K_i, z) &= w(K_p^0, K_i^0, z) + \frac{\partial w(K_p^0, K_i^0, z)}{\partial K_p}\Delta K_p \\ &\quad + \frac{\partial w(K_p^0, K_i^0, z)}{\partial K_i}\Delta K_i + \cdots \end{aligned} \tag{3.1}$$

where

$$\frac{\partial w(K^0, z)}{\partial K} \triangleq \text{sensitivity of the output } w(K^0, z)$$
$$\text{with respect to the parameter K at } K = K^0.$$

If the expression is truncated to the first-order term, $w(K_p^0, K_i^0, z)$ is defined as the nominal response of the system, and $w(K_p^0 + \Delta K_p, K_i^0 + \Delta K_i, z)$ is used as the desired response of the system, then the error between the desired and nominal responses can be approximated by

$$e(z) \cong \frac{\partial w(K_p^0, K_i^0, z)}{\partial K_p}\Delta K_p + \frac{\partial w(K_p^0, K_i^0, z)}{\partial K_i}\Delta K_i. \tag{3.2}$$

This approximation implies that, given the knowledge of the error and of the sensitivity functions, the values of ΔK_p and ΔK_i can be found such that when added to K_p and K_i, the error will be reduced.

The error used in Equation (3.2) can be generated with the use of a reference model. The sensitivity functions can be generated by the system itself, or by an appropriate sensitivity model with sensitivity filters.

Again consider Figure 3.1. The system transfer funtion is given by

$$w(z) = \frac{C(z)G(z)}{1 + C(z)G(z)}r(z) = H(z)r(z). \tag{3.3}$$

Now the sensitivity of the output with respect to the parameter K is given by

$$\frac{\partial w}{\partial K} = \frac{\partial H(z)}{\partial K} r = \frac{1}{H(z)} \frac{\partial H(z)}{\partial K} H(z) r = \frac{\partial \ln H(z)}{\partial K} w. \tag{3.4}$$

For sensitivity guided design, the logarithmic sensitivity function

$$\frac{\partial w}{\partial \ln K} = K \frac{\partial w}{\partial K} \tag{3.5}$$

is more practical because it gives the change in the output for a given relative change in K. However, for the automatic tuning methods, the sensitivity function given in Equation (3.4) is generally used. For completeness, both types are developed here.

Multiplying Equation (3.4) by K gives

$$K \frac{\partial w}{\partial K} = \frac{\partial w}{\partial \ln K} = \frac{\partial \ln H(z)}{\partial \ln K} w. \tag{3.6}$$

Now

$$\frac{\partial \ln H(z)}{\partial \ln K} = \frac{\partial \ln H(z)}{\partial \ln C(z)} \frac{\partial \ln C(z)}{\partial \ln K} = S_C F_K \tag{3.7}$$

where S_C represents the sensitivity model, and F_K represents the sensitivity filter of the parameter K. Solving explicitly for S_C and F_K gives

$$S_C = \frac{\partial \ln H(z)}{\partial \ln K} = C(z) \frac{\partial}{\partial C(z)} \ln \left[\frac{GC}{1+GC} \right] = \frac{1}{1+GC} \tag{3.8}$$

and

$$F_K = \frac{\partial \ln C(z)}{\partial \ln K} = K \frac{\partial \ln C(z)}{\partial K}. \tag{3.9}$$

For the PI controller,

$$F_{K_p} = K_p \frac{\partial}{\partial K_p} \ln \left[K_p + \frac{K_i T}{z-1} \right] = \frac{1}{C(z)} K_p \tag{3.10}$$

and similarly for K_I,

$$F_{K_i} = \frac{1}{C(z)} \frac{K_i T}{z-1}. \tag{3.11}$$

The final forms of the sensitivity functions are then

$$\frac{\partial w}{\partial K_p} = \frac{1}{1+GC}\frac{1}{C(z)}w \tag{3.12}$$

$$\frac{\partial w}{\partial K_i} = \frac{1}{1+GC}\frac{1}{C(z)}\frac{T}{z-1}w \tag{3.13}$$

and for the logarithmic sensitivity functions,

$$\frac{\partial w}{\partial \ln K_p} = K_p\frac{\partial w}{\partial K_p} \tag{3.14}$$

$$\frac{\partial w}{\partial \ln K_i} = K_i\frac{\partial w}{\partial K_i}. \tag{3.15}$$

It should be noted that these functions are valid only if the pole of $1/C(z)$ is strictly stable. This condition forces the controller to have a strictly minimum phase zero.

Figure 3.2 shows the block diagram of a system that could be used to generate these sensitivity functions. The signal labeled S_C in the diagram is denoted as the "sensitivity point" of the system and can be easily generated for use in calculating the sensitivity functions.

3.2 Sensitivity Function Example

In order to illustrate the usefulness of sensitivity functions in the design of systems, an example is given. Again, consider the system shown in Figure 3.2 with

$$G(z) = \frac{-0.0006z^2 - 0.0032z - 0.0006}{z^4 - 1.0658z^3 + 0.01z^2 + 0.0383z + 0.1340} \tag{3.16}$$

as the transfer function from the travel rate reference input to the puddle width output.

The step response of the reference model (the desired response) and system, and the output sensitivity functions with respect to percent changes in K_p and K_i are shown in Figure 3.3.

The most prominent characteristic of the sensitivity functions shown in this plot is that the output is considerably more sensitive to changes in K_i than to changes in K_p.

As was implied by Equation (3.1), the sensitivity functions can be used to approximate the new response of the output after the parameters are adjusted. The goal in Figure 3.3 is to change K_p and K_i in a way such that the new output response will be close to the desired response. An examination of the plots suggests that K_p be increased by 50%, and K_i be increased by 25%. The new output response would then be approximated to the first order by

$$\text{new width} = \text{old width} + 0.5\frac{\partial w}{\partial \ln K_p} + 0.25\frac{\partial w}{\partial \ln K_i}. \tag{3.17}$$

Figure 3.4 shows the desired response, the actual new response, and the approximated new response. As can be seen, the approximated new response is very close to the actual new response. Roughly speaking, the approximated response will be very close to the estimated response as long as the parameters are not varied by more than about 50% of their value.

The output could be further tuned to the desired response by iteratively repeating the above procedure. This type of approach is sometimes known as Sensitivity Guided Design (SGD).

3.3 Automatic Tuning Methods

There are a variety of methods available to automatically tune the parameters using some output error and the output sensitivity functions. They are divided into two main catagories, off-line tuning and on-line tuning. In off-line tuning, special inputs may be needed, and, hence, the parameters are tuned while the plant or system is not operating. In on-line tuning, no special inputs are used, and the parameters are tuned while the system is in uninterrupted operation.

3.3.1 Off-line tuning

In off-line tuning, the system itself can be used to generate the sensitivity point signal, and, hence, the amount of required system modeling is reduced. The needed parameter changes, ΔK_p and ΔK_i, are calculated to minimize some cost functional using a least-squares or gradient algorithm, in general.

For off-line tuning, the sensitivity functions can be generated from two consecutive system runs. The first run is used to generate the system output response. The second run applies this response as a new system input and gives the sensitivity point signal as its output. The sensitivity point signal is then passed through the appropriate known sensitivity filters to produce the sensitivity functions. The sensitivity filters are known because the structure of the controller is known. One of the nice characteristics of off-line tuning is that the plant does not have to be known in order to generate the true sensitivity functions. In other words, it is possible to use the actual system to generate both the system output and the sensitivity point signal.

Least-Squares Estimation

Suppose it is desired that the system respond in the same manner to a step input as a particular reference model. Let w_{ref} be the output of the reference model and w be the output of the system. Then the output error can be defined as

$$e_o = w_{\text{ref}} - w. \tag{3.18}$$

Define the cost functional to be minimized as

$$J = \frac{1}{2} \sum_{i=0}^{N-1} (e_o(iT))^2. \tag{3.19}$$

The time domain couterpart of Equation (3.2) is

$$e_o(iT) = \Delta K_p \frac{\partial w(iT)}{\partial K_p}\bigg|_{K_p(iT)K_i(iT)} + \Delta K_i \frac{\partial w(iT)}{\partial K_i}\bigg|_{K_p(iT),K_i(iT)}. \tag{3.20}$$

Over a period of N intervals, this single equation gives rise to an over-determined system of equations in the two unknowns $\Delta K_p, \Delta K_i$ given by

$$\begin{bmatrix} e_o(0) \\ \vdots \\ e_o((N-1)T) \end{bmatrix} = \begin{bmatrix} \frac{\partial w(0)}{\partial K_p} & \frac{\partial w(0)}{\partial K_i} \\ \vdots & \vdots \\ \frac{\partial w((N-1_T))}{\partial K_p} & \frac{\partial w((N-1)T))}{\partial K_i} \end{bmatrix} \begin{bmatrix} \Delta K_p \\ \Delta K_i \end{bmatrix} \tag{3.21}$$

which in matrix notation gives

$$E = S\,\Delta K \tag{3.22}$$

where E is an $N \times 1$ vector of error points, S is an $N \times 2$ matrix of sensitivity function points, and ΔK is a 2×1 vector of unknown parameter adjustments. Multiplying both sides of Equation (3.22) by the transpose of S

$$S^T E = S^T S \Delta K \tag{3.23}$$

and solving for ΔK gives

$$\Delta K = (S^T S)^{-1} S^T E \tag{3.24}$$

which is the least-squares solution to Equation (3.22), provided $S^T S$ is invertible. This solution always applies for two or less parameters, but for three or more, the columns of S may be linearly dependent, and another method would have to be used [21]. Using the results from Equation (3.24), the new parameters would be

$$K_{\text{new}} = K_{\text{old}} + \epsilon \Gamma \Delta K \tag{3.25}$$

where ϵ is the parameter update step size, and Γ is a matrix used to weight the relative step sizes between the two parameters. The values for these constants in a particular system are generally determined through trial-and-error experiments.

Gradient Estimation

The gradient algorithm for the minimization of Equation (3.19) is even simpler and is given by

$$K_{\text{new}} = K_{\text{old}} - \epsilon\Gamma\nabla_K J = K_{\text{old}} + \epsilon\Gamma\Delta K \tag{3.26}$$

where

$$\nabla_K J = \frac{\partial}{\partial K}\frac{1}{2}\sum_{i=0}^{N-1}(e_o(iT))^2 = \begin{bmatrix} \sum_{i=0}^{N-1} e_o(iT)\frac{\partial e_o(iT)}{\partial K_p} \\ \sum_{i=0}^{N-1} e_o(iT)\frac{\partial e_o(iT)}{\partial K_i} \end{bmatrix}. \tag{3.27}$$

Taking the partial derivative of Equation (3.18) with respect to parameter K gives

$$\frac{\partial e_o(iT)}{\partial K} = -\frac{\partial w(iT)}{\partial K}. \tag{3.28}$$

Using Equation (3.28) in Equation (3.27) and rewriting in matrix notation gives

$$-\nabla_K J = \Delta K = S^T E \tag{3.29}$$

where ΔK, S, and E are defined as before. This algorithm will work for any number of parameters, but in the case where the sensitivity funtions are linearly independent its convergence will be slow.

3.3.2 On-line tuning

As was mentioned earlier, on-line tuning of the controller parameters is performed while the system is in operation. This method is also known as "self-tuning control" or "direct adaptive control." There are two main groups of direct adaptive controllers of this type, ones that update the parameters periodically, and ones that update them at every time sample.

The adaptive systems that update the parameters periodically are basically the same as the off-line automatic tuning systems except that the sensitivity model and filters used

to generate the sensitivity functions are run concurrently with the system. The sensitivity model in this case is only a rough approximation of the true system.

The adaptive system presented here updates the parameters at every time sample using a steepest-descent pseudo-gradient parameter update law. A block diagram of this type of system is given in Figure 3.5.

It should be noted that the implementation of the inverted controller in this particluar scheme has K_p and K_i fixed at their simulated optimum values ($K_p = -0.1186$, $K_i = -0.0640$, simulated without noise). This is done for two practical reasons. First, it avoids the need for implementing a highly non-linear system for the inverted controller. Second, it disposes of the condition that states that the zero of the controller must be minimum phase. The pole of the inverted controller for these gains is strictly stable.

The reason that this is considered to be a pseudo-gradient method instead of a gradient method is that the sensitivity functions generated are only approximations of the true ones. This is a result of the use of a model in place of the plant in the sensitivity model, and of the use of a fixed-gain inverted controller in the sensitivity filters. Whenever an approximation of the system is used as the sensitivity model, the resultant sensitivity functions will be called pseudo-sensitivity functions and the sensitivity model will be known as the pseudo-sensitivity model.

The parameter update law for this system is given by

$$K_{i+1} = K_i - \epsilon \Gamma T \nabla_K J \tag{3.30}$$

where i is the time index, and T is the sample period. The cost functional for this method is given by

$$J = \frac{1}{2}(e_o(iT))^2. \tag{3.31}$$

This cost functional minimizes the square of the output error at each point in time, instead

of over a period as in the off-line case. However, the averaging and slow adaptation results given in [19,18,22] show that in the average sense the adaptive system presented here will minimize the square of the output error over a period.

Now the gradient of J with respect to the parameters is

$$\nabla_K J = \left(e_o(iT) \frac{\partial e_o(iT)}{\partial K} \right) \cong - \left(e_o(iT) \frac{\partial \tilde{w}\,(iT)}{\partial K} \right) \tag{3.32}$$

where

$$\frac{\partial \tilde{w}\,(iT)}{\partial K} \triangleq \text{pseudo-sensitivity of the output } w(K^0, z) \text{ with respect to the parameter K at } K = K^0.$$

In order to ensure that this adaptive system will be stable, a few conditions must be met [22]. First, the parameters must change slowly with respect to the system dynamics. In other words, the step size, ϵ, in the update law must be small.

The second condition states that the pseudo-sensitivity model must be chosen such that the pseudo-sensitivity functions are never more than $\pm 90°$ out of phase with the true sensitivity functions. If the approximate sensitivity functions used in calculating Equation (3.30) were more than $\pm 90°$ out of phase with the true sensitivity functions, Equation (3.30) would in effect be the "steepest-ascent" update law for the parameters. More precisely, this would cause a positive-feedback effect in the parameter update law, which in turn would cause the system to drift towards instability.

These conditions for stability are necessary and sufficient for this type of system. For a more complete derivation and analysis of adaptive systems of this type see [22].

3.4 The Problem of Noise

In many adaptive control systems, noise can present a serious problem. Usually, it causes the parameters of a system to drift away from their tuned values, possibly causing

instability. However, using the sensitivity method, there are situations in which the noise in a system can be interpreted in such a way that it will not pose a significant problem. This is the case in this application.

Consider the block diagram of the puddle width control system with noise given in Figure 3.6a. Because of the locations of the noise disturbances present in the system, they can be considered as additional system inputs as shown in Figure 3.6b. If the noise was present in, or just before, the controller block, this would no longer be the case. The reason for this is that the location of the tunable parameters, which represent a non-linearity in the system, prohibits the use of superposition with regard to the noise input.

Sensitivity functions generated from a multiple-input system like the one shown in Figure 3.6b are true sensitivity functions with respect to a different input. In general, they lead to different tuning results [22]. The reason for this is because the output error for the multi-input case is not the same as the one for the single-input case. The on-line adaptive system works to minimize the square of the output error and will therefore lead to different parameter equilibria for different inputs.

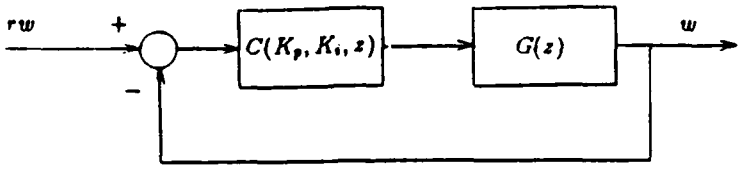

Figure 3.1 Width control system.

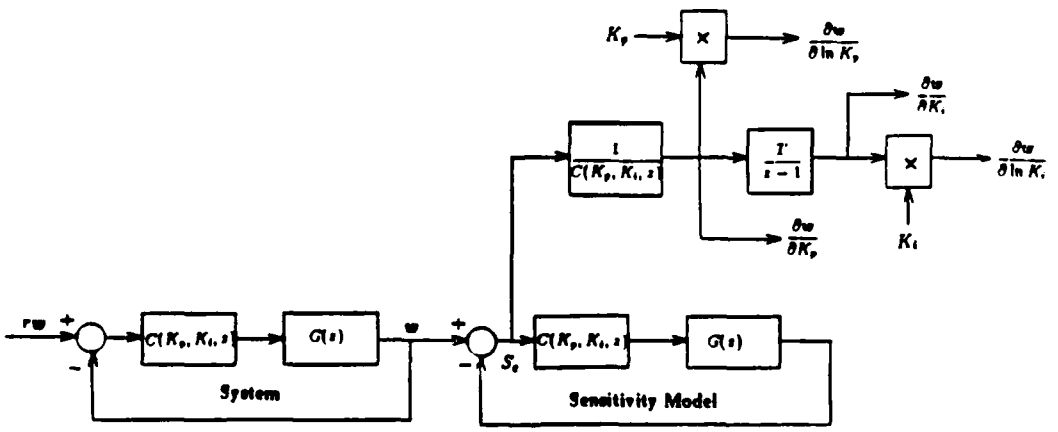

Figure 3.2 System used to generate sensitivity functions.

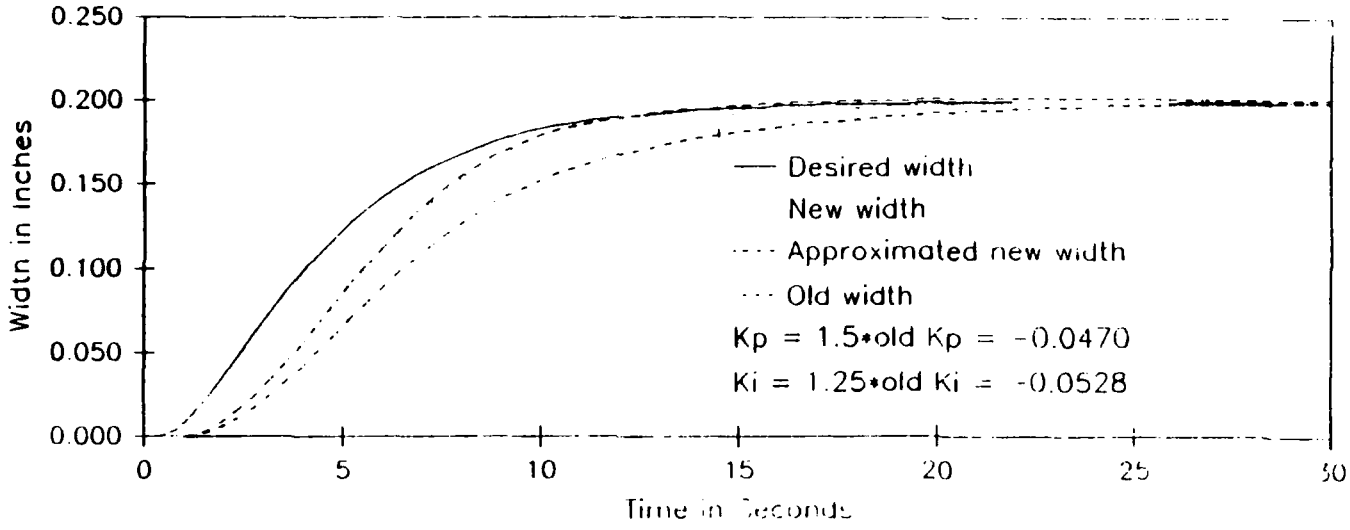

Figure 3.3 Example step responses and sensitivity functions.

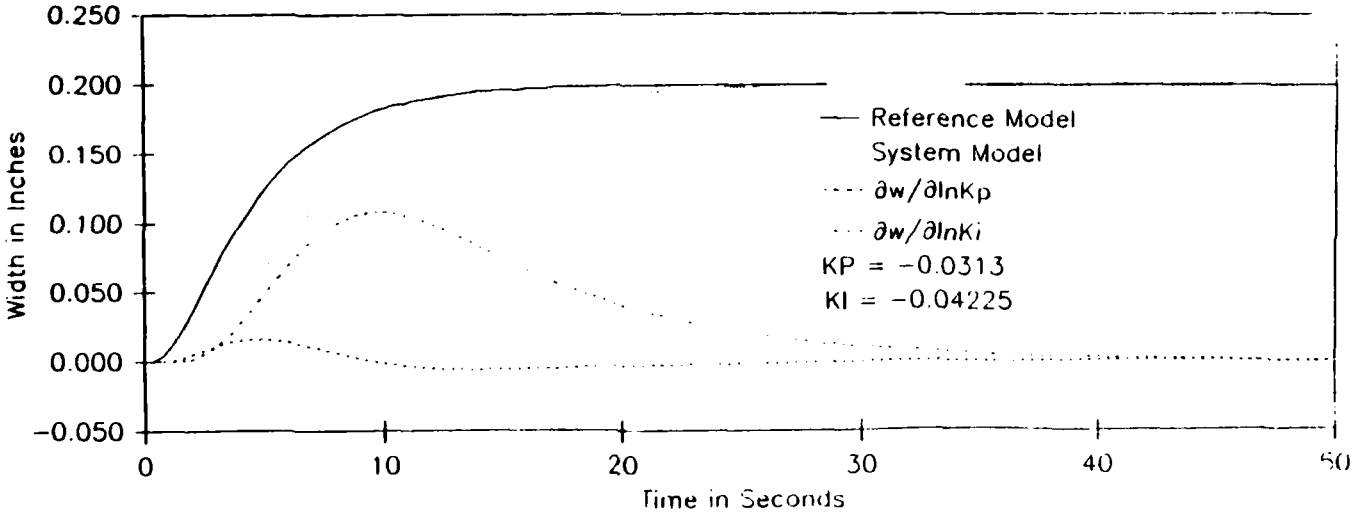

Figure 3.4 Actual and approximated step responses compared with old step response.

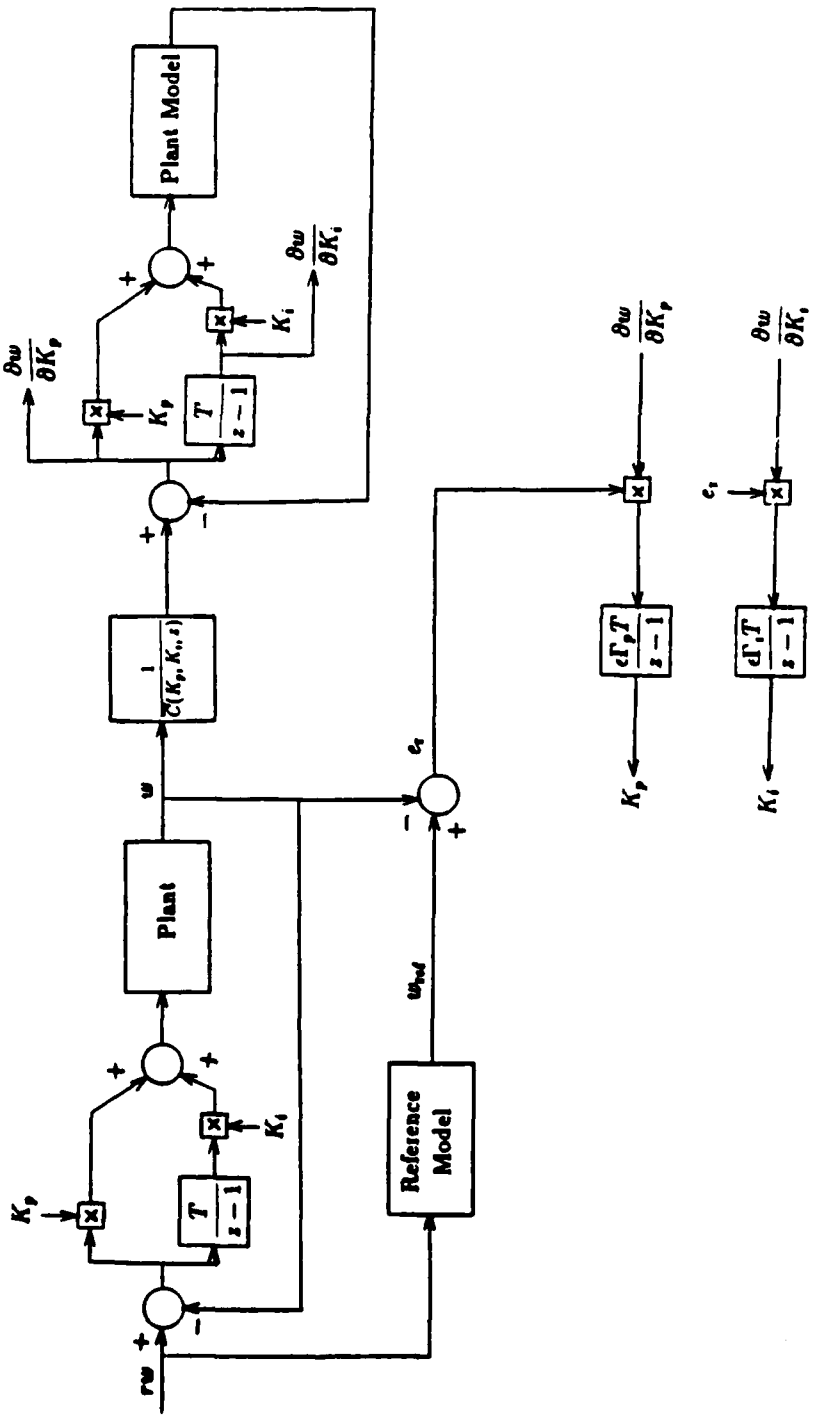

Figure 3.5 On-line adaptive system using pseudo-gradient parameter update law.

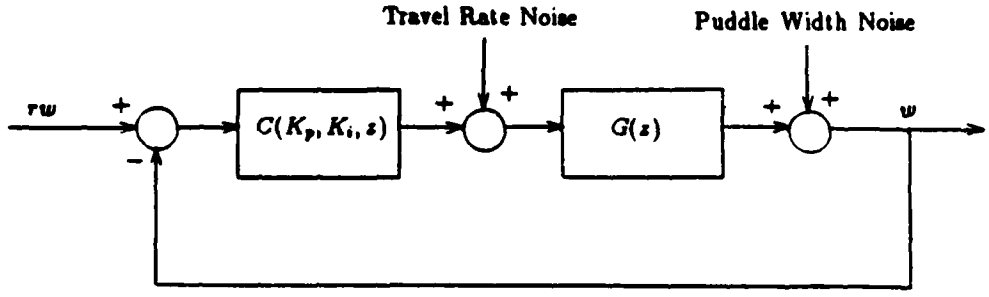

(a)

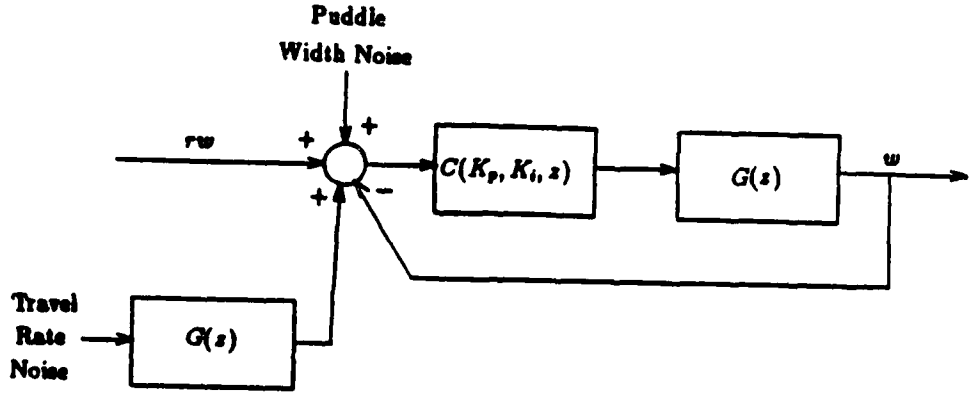

(b)

Figure 3.6 Treatment of noise in the system. (a) Width control system with noise. (b) System with noise considered as additional inputs.

CHAPTER 4

OFF-LINE TUNING: SIMULATIONS

Off-line tuning simulations examine the usefulness of off-line automatic tuning. They also provided the author with the preliminary experience needed to implement on-line tuning. The first simulation gives the results using least-squares estimation for determining the needed parameter changes. The second one gives the same type of results using gradient estimation.

Systems which are linear, or are non-linear but used near an operating point, and which do not vary with time are good candidates for the application of these off-line tuning methods. Because the welding system presented here is used over a wide range of operating points, this type of tuning is not well-suited to it and was therefore not implemented.

Figures 4.1(a) and 4.1(b) show the block diagram of the system used for simulating the off-line tuning methods. As was discussed earlier, the system was run twice in order to generate the information needed to update the parameters. In the first run, shown in Figure 4.1(a), the puddle width and output error signals were generated. In the second run, shown in Figure 4.1(b), the sensitivity functions were generated using the puddle width signal from the first run as the input. The noise added to the system was random noise with a magnitude of $\pm$ 10% of the output, plus a constant term with a magnitude of -25%

of the output. The random noise was designed to be different for each run of the system. This was done to ensure that the noise would be different between the first and second runs of the system, and between successive tuning iterations. The initial conditions of the controller gains for these simulations were chosen to be $K_p^0 = -0.07$ and $K_i^0 = -0.25$. With these gains the system is unstable. Figure 4.2 shows the step response of the system with these gains and of the reference model. All simulations were done using Matrix_x.

4.1 Least-Squares Simulation

The purpose of this simulation is to demonstrate the performance of least-squares estimation in updating the parameters in an off-line tuning system. The step size for this simulation was $\epsilon = 1$, and the weighting matrix was

$$\Gamma = \begin{bmatrix} 500 & 0 \\ 0 & 1000 \end{bmatrix}.$$

The simulation consisted of 100 tuning iterations. In each iteration, the system was run twice.

The parameters were found to have converged after 20 iterations. Table 4.1 gives the tuning history of the simulation. Figure 4.3 shows the step responses of the tuned system and of the reference model. As can be seen, the response of the tuned system very closely matches that of the reference model. However, the number of iterations taken to arrive at this response is high.

4.2 Gradient Simulation

The purpose of this simulation is to demonstrate the performance of gradient estimation in updating the parameters in an off-line tuning system. For this simulation, the step size

was $\epsilon = 10^{-5}$, and the weighting matrix was

$$\Gamma = \begin{bmatrix} 50 & 0 \\ 0 & 5 \end{bmatrix}.$$

The simulation consisted of 25 iterations of two runs each.

The parameters were found to have converged after only one iteration. Table 4.2 gives the tuning history for this simulation. Figure 4.4 shows the response of the tuned system and of the reference model. The response of this tuned system is acceptable, but not as good as the least-squares response in Figure 4.3. This approach took only one iteration to converge, which is quite an improvement over the least-squares approach. Of the two, the gradient method would be the one to use in this application if off-line automatic tuning was to be implemented.

Another alternative would be to use a combination of the two algorithms, using perhaps the gradient algorithm for the first few tuning iterations, and then finishing with the least-squares method. This type of approach was not simulated, but would be worth investigating in the application of off-line tuning.

Table 4.1 LSE simulation tuning history.

Iteration	K_p	K_i
0	-0.0704	-0.2500
1	-0.0628	-0.2366
2	-0.0547	-0.2228
3	-0.0459	-0.2078
4	-0.0365	-0.1912
5	-0.0249	-0.1737
6	-0.0120	-0.1532
7	0.0043	-0.1285
8	0.0242	-0.0995
9	0.0448	-0.0695
10	0.0619	-0.0465
11	0.0590	-0.0314
12	0.0352	-0.0225
13	-0.0377	-0.0252
14	-0.1445	-0.0507
15	-0.1360	-0.0676
16	-0.1131	-0.0689
17	-0.0970	-0.0645
18	-0.0862	-0.0621
19	-0.0839	-0.0612

Table 4.2 Gradient simulation tuning history.

Iteration	K_p	K_i
0	-0.0704	-0.2500
1	-0.0152	-0.0629

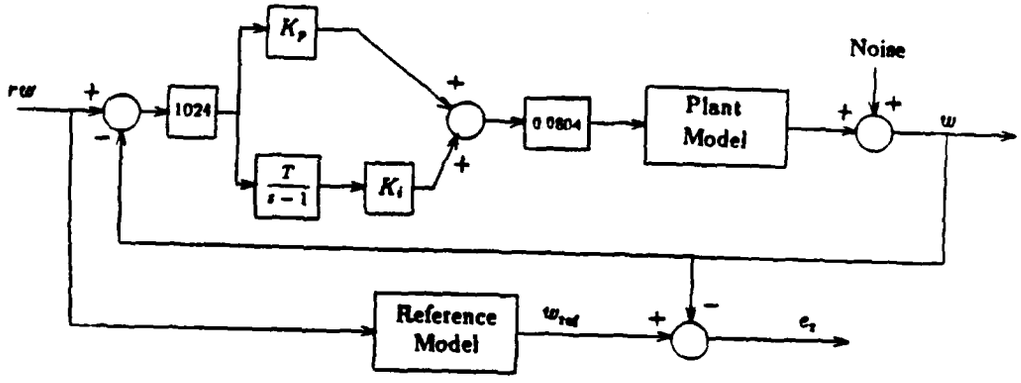

(a)

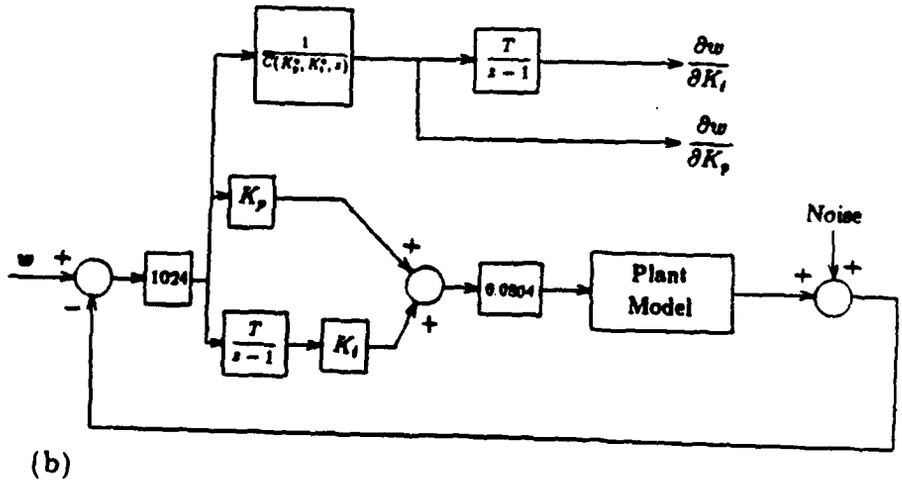

(b)

Figure 4.1 System to simulate off-line tuning. (a) First system run. (b) Second system run.

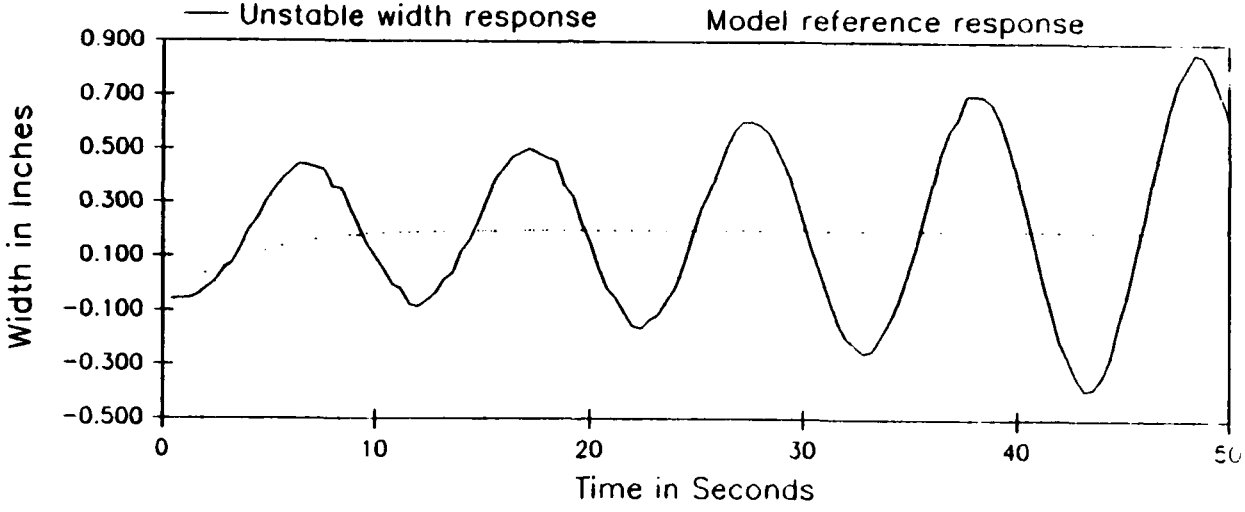

Figure 4.2 Step response of the unstable system.

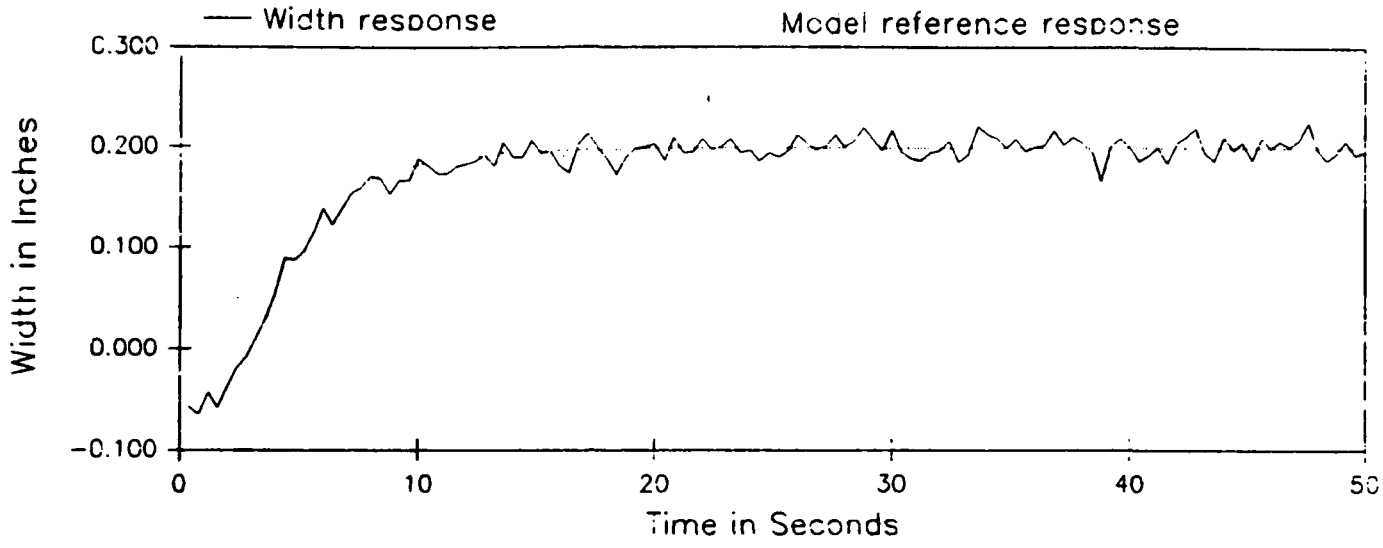

Figure 4.3 Step response of system tuned using least-squares estimation.

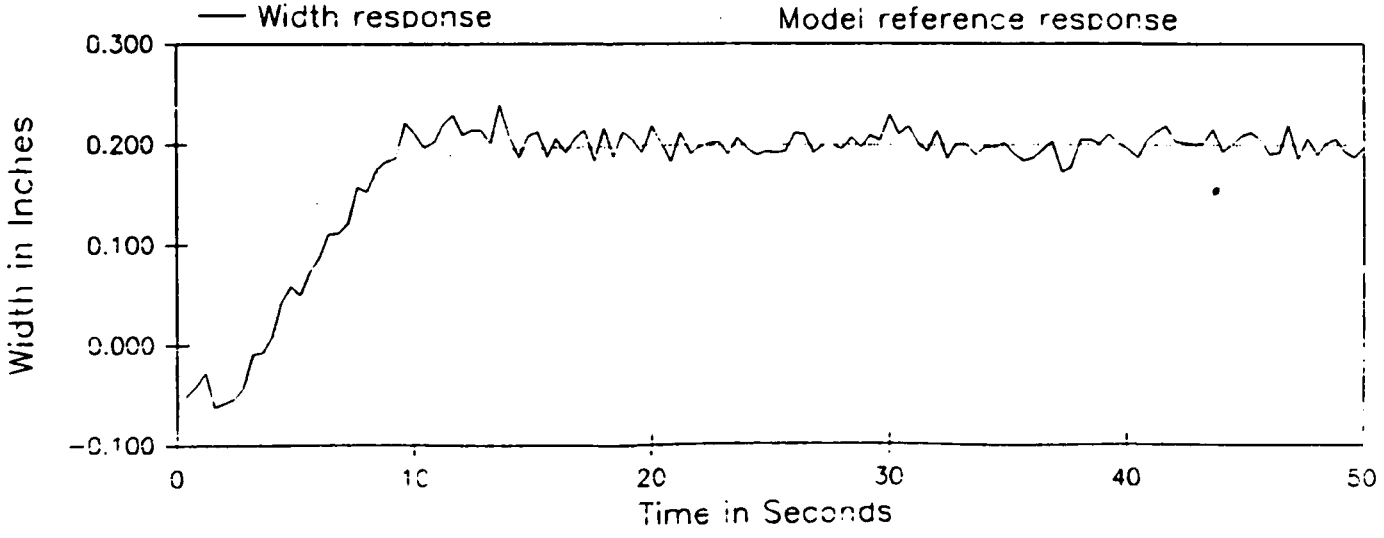

Figure 4.4 Step response of system tuned using gradient estimation.

CHAPTER 5

ON-LINE TUNING: SIMULATIONS AND EXPERIMENTS

The results of simulations and experiments presented in this chapter demonstrate the usefulness and robustness of the designed direct adaptive control system in the control of weld puddle width.

All of the reasons given in Chapter 4 for avoiding automatic off-line tuning of the welding system are good reasons for using on-line tuning. An on-line adaptive system is needed for the welding system because of its large operating range. It would be useful for retuning the puddle width controller when the operating conditions change. The adaptive system presented here is well-suited for tuning the simple PI controller at the different operating points of the non-linear welding system.

The simulations in this chapter demonstrate the robustness of this system to variations in the plant dynamics while the pseudo-sensitivity model remains the same. The experimental results given in this chapter confirm those predicted by the simulations, with a few exceptions.

5.1 Simulations

The purpose of these simulations is to examine the convergence of the adaptive system and the performance of the tuned puddle width response in spite of the presence of noise and variations in the plant. Figure 5.1 gives the block diagram of the system used for these simulations. The nominal current plant model given in Chapter 2 is used to model the plant in the pseudo-sensitivity model for all of these simulations. The transfer function for the inverted controller is

$$\frac{1}{\overline{C}(z)} = \frac{z-1}{-0.1186z + 0.093}. \tag{5.1}$$

In the first simulation, the nominal-current plant model was used to model the plant in the system model, in the second, the high-current model was used, and in the third, the low-current model was used. The update law parameters for these simulations were

$$\epsilon = 7.5 \times 10^{-6}$$

$$\Gamma = \begin{bmatrix} 1 & 0 \\ 0 & 1 \end{bmatrix}.$$

The initial controller gains were chosen such that the system would start out unstable. The noise introduced into the system was random noise with a magnitude of $\pm$ 10% of the output plus a constant term with a magnitude of -50% of the output.

Figures 5.2 through 5.4 show the puddle width responses and parameter convergence histories for the three simulations.

Figure 5.2(a) shows the input, model reference response, and the puddle width response for the case where the nominal-current plant model is used in the system model. As can be seen, the system is nicely tuned in less than one minute. Figure 5.2(b) gives the parameter convergence history for this case. It should be noted that the noise does not seem to cause any problems in the convergence of the parameters.

Figure 5.3(a) gives the input and responses for the case where the system model uses the high-current plant model. The system does not tune to the final parameter values as fast as it did in the first case, but it is stabilized in less than one minute. Figure 5.3(b) shows the parameter convergence history for this case.

Figure 5.4(a) shows the input and responses for the case where the low-current plant model is used in the system model. Again the tuning is not as good as it was in the first case, but the system is stabilized in less than a minute. Figure 5.4(b) gives the parameter convergence plot for this case.

Figure 5.5(a) shows the output sensitivity functions with respect to K_p and K_i for the first case simulation. Figure 5.5(b) shows these experimental results and will be discussed later. There are two observations to be made from this figure. The first is that the relative magnitude difference between the sensitivity functions indicates that the integral gain has a much larger effect on the puddle width than does the proportional gain. The second observation is that the noise primarily seems to affect the proportional gain sensitivity function. These two results taken together help the robustness of the system because the parameter that carries the most weight is least affected by noise.

Overall, the simulations predict that the adaptive system will perform well in the presence of noise and for anticipated variations in the plant.

5.2 Experiments

The purpose of these experiments is to demonstrate the value and robust performance of this direct adaptive puddle width control system. Figure 5.6 gives a block diagram of the implemented on-line tuning system. The nominal-current plant model given in Chapter 2 was used in the pseudo-sensitivity model for all of these experiments. The initial controller gains were chosen such that the system was initially unstable ($K_p = -0.0704$, $K_i = -0.15$).

For all of these experiments, the step size was $\epsilon = 7.5 \times 10^{-6}$, and the weighting matrix was

$$\Gamma = \begin{bmatrix} 1 & 0 \\ 0 & 1 \end{bmatrix}.$$

Six experiments were conducted over most of the operating range of the welding system. Table 5.1 lists the experiments and their corresponding operating points. The power supply voltage, shield gas composition and flow rate, and contact tube height were identical for all experiments. The values for these variables are given in the Appendix . In each experiment, a single bead was deposited on a 48″ × 16″ steel plate. The first three experiments were done on a 1″ thick plate, the last three on a $\frac{1}{2}$″ thick plate. Prior to each experiment, the plate was preheated to 250° F by raising the surface temperature to 300° F, and allowing the plate to passively cool. As the plate cools, the surface temperature along the weld line is allowed to become uniform to within 15° F before the experiment is started. This procedure is necessary since puddle geometry is affected by the initial plate temperature [10]. A hand-held thermo sensor (Material Controls, model FXP 2000 Thermo Sensor) was used to monitor the plate temperature.

Figures 5.7 through 5.12 show the results from these experiments. Part (a) of the figures gives the input, reference model response, and puddle width response. Part (b) of the figures gives the parameter convergence history.

Figures 5.7 through 5.9 show the results from the experiments run on the 1" thick plate. The high magnitude of the noise in the puddle width responses in general suggests that the noise used in the simulations underestimated the true system noise. In all three of the experiments, however, the system was tuned close to the reference model in less than one minute. An interesting result is given in the parameter convergence plots of these figures. For all three experiments, the parameters converged towards the same tuned values. This result was not expected, since the models describing the dynamics of the system at these

three operating points are so different. The simulations predicted that the parameters would converge to different equilibria for different operating points in the presence of a relatively small amount of noise. A possible reason that this did not occur in the real system might be that the noise present in the system is of large enough magnitude that its influence overshadowed the effects of the plant variations in the parameter tuning.

Figures 5.10 through 5.12 show the results from the experiments performed on the $\frac{1}{2}''$ thick plate. The dynamics of the puddle geometry on the thinner plate are much different from those on the 1" plate. Because of this, it is known that the plant model used in the pseudo-sensitivity model for this adaptive system does not match the plant in any of the thin plate operating points. In spite of this large mismatch, the puddle width responses in these figures show that the adaptive system performs well. In all three experiments, the system is tuned in about the same amount of time as in the thick plate experiments. The parameter convergence results for these experiments are in closer agreement to what the simulations suggested might be expected. In each experiment, the parameters converge towards a different equilibrium. Following the same line of reasoning as given for the thick plate parameter convergence, this result may have occurred because the effects of the mismatch between the true plant and the sensitivity model had a greater influence on the parameter convergence than the effects the noise had.

Figure 5.5(b) shows the parameter sensitivity functions for the nominal operating point. When compared with the simulated sensitivity functions for this operating point shown in Figure 5.5(a), it can be seen that they are very similar. The conclusions that were drawn from the simulated sensitivity functions could also be drawn from the real ones. Namely, that the integral gain has the greater effect on the output, and that the proportional gain sensitivity function is most affected by the noise present in the system.

Figures 5.13 through 5.15 give the comparisons between the simulated and experimental

results for the three operating points on the 1" thick plate. As can be seen, the simulations give a fair prediction of the actual responses of the system. As was mentioned earlier, the noise in the actual system is much worse than that used in the simulations, and may account for some of the differences between the simulated and experimental results.

In general, these experiments demonstrate the versatility and robustness of this adaptive puddle width control system. The system performed well in the presence of heavy noise over a wide range of operating conditions.

Table 5.1 Experiments and corresponding operating points.

Experiment	Arc Current (A)	Plate Thickness (in)
1	360	1
2	330	1
3	390	1
4	360	1/2
5	330	1/2
6	390	1/2

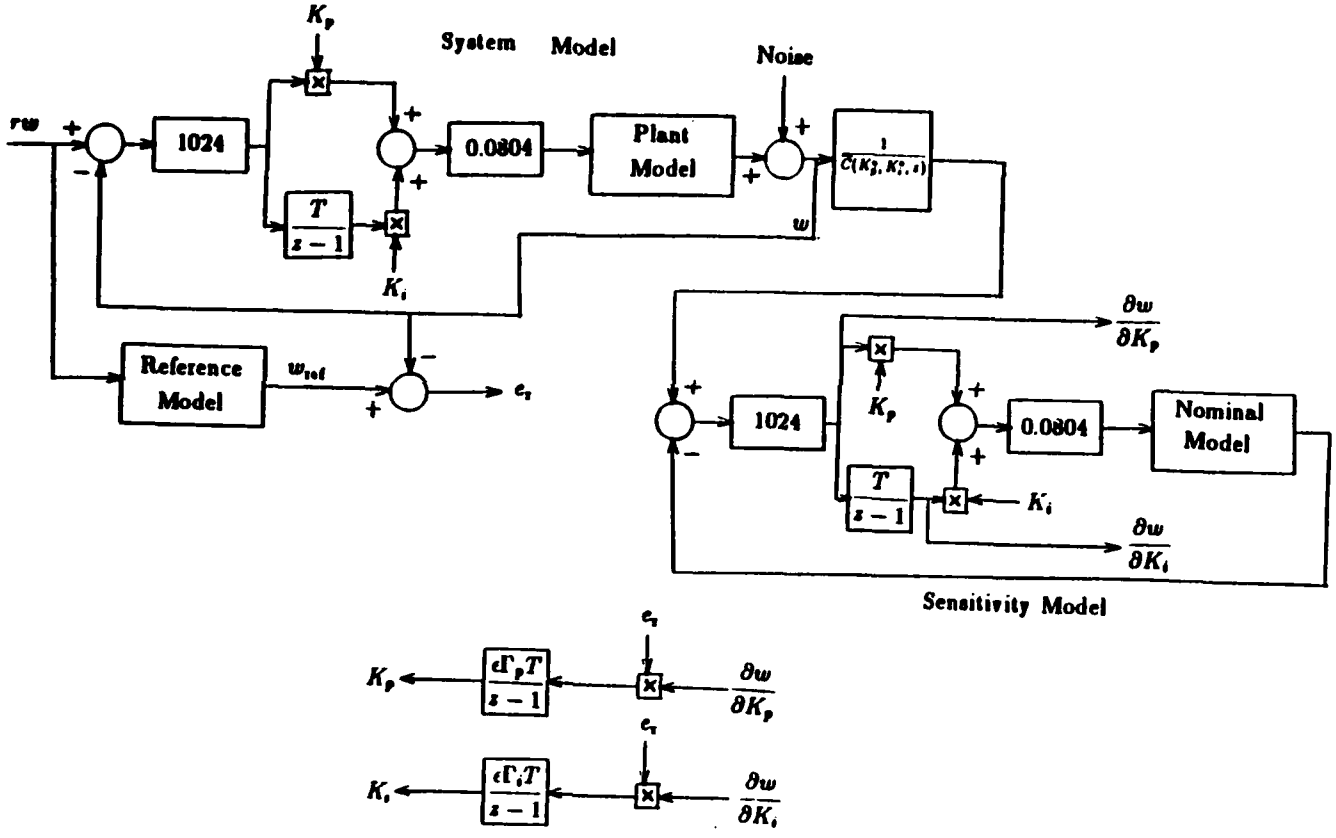

Figure 5.1 Block diagram of system used in simulations of on-line system.

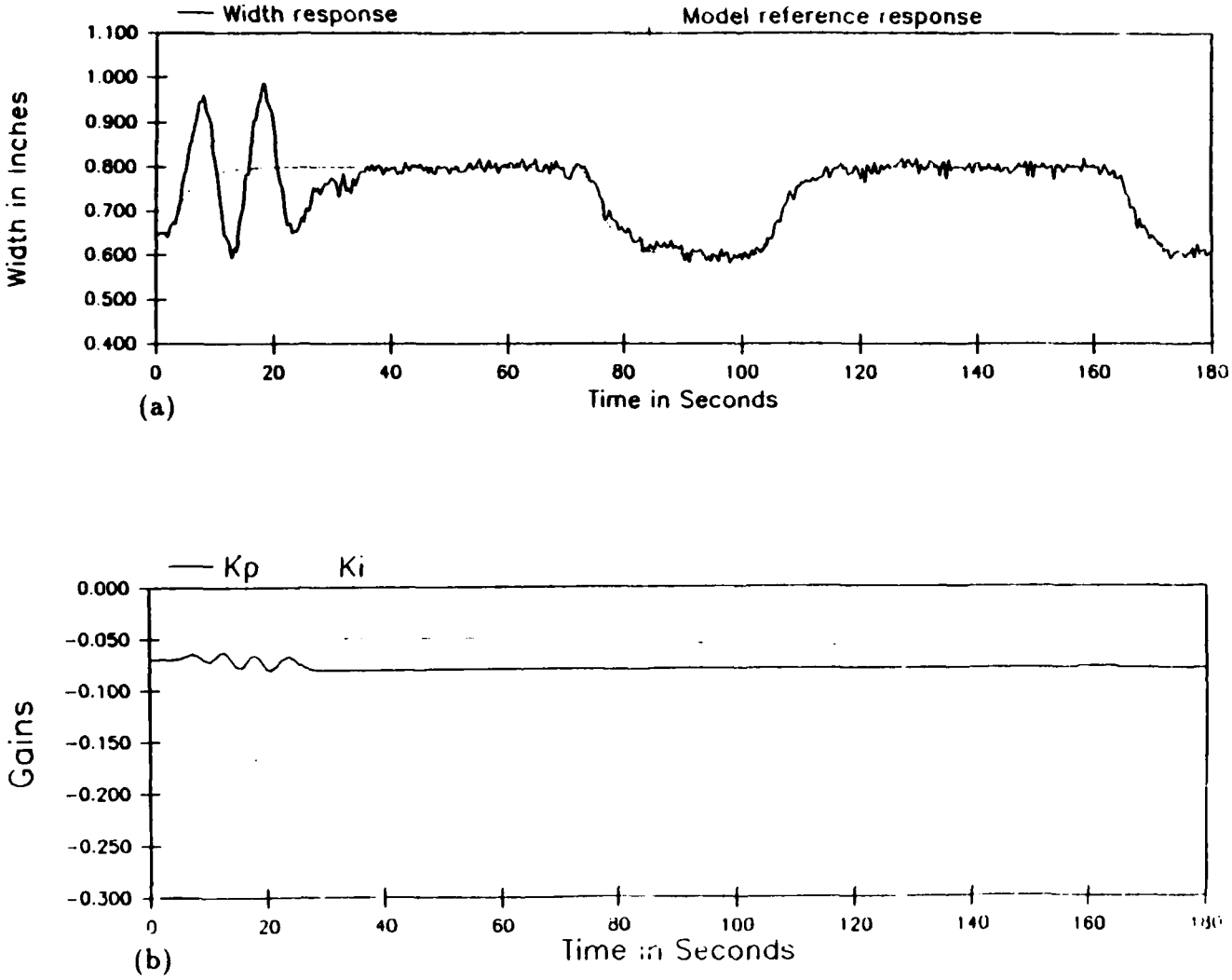

Figure 5.2 Results of simulation with operating point at 360 A, 1" thick plate. (a) Width response. (b) Parameter Convergence.

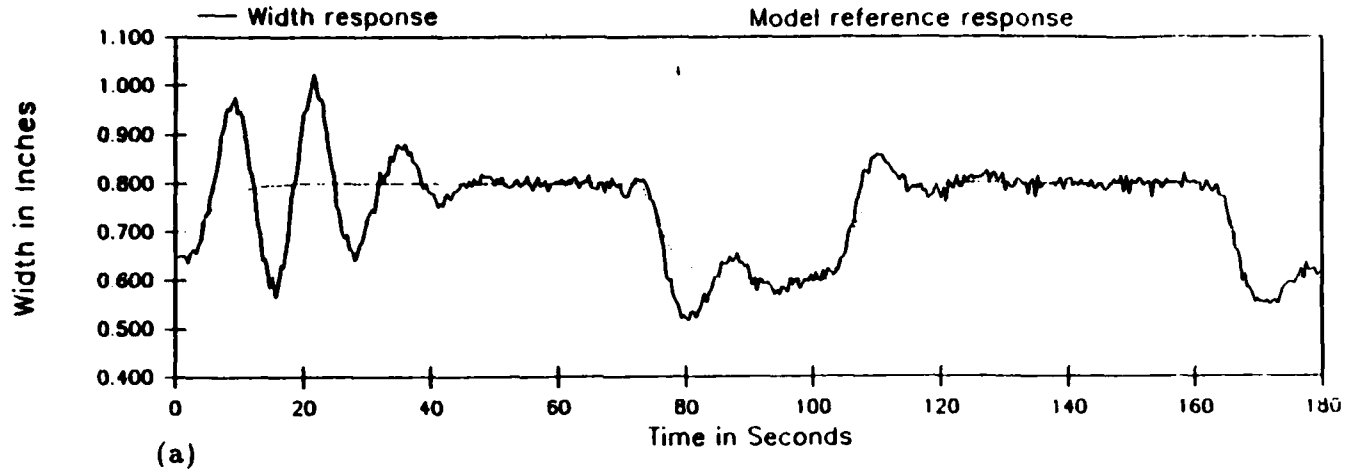

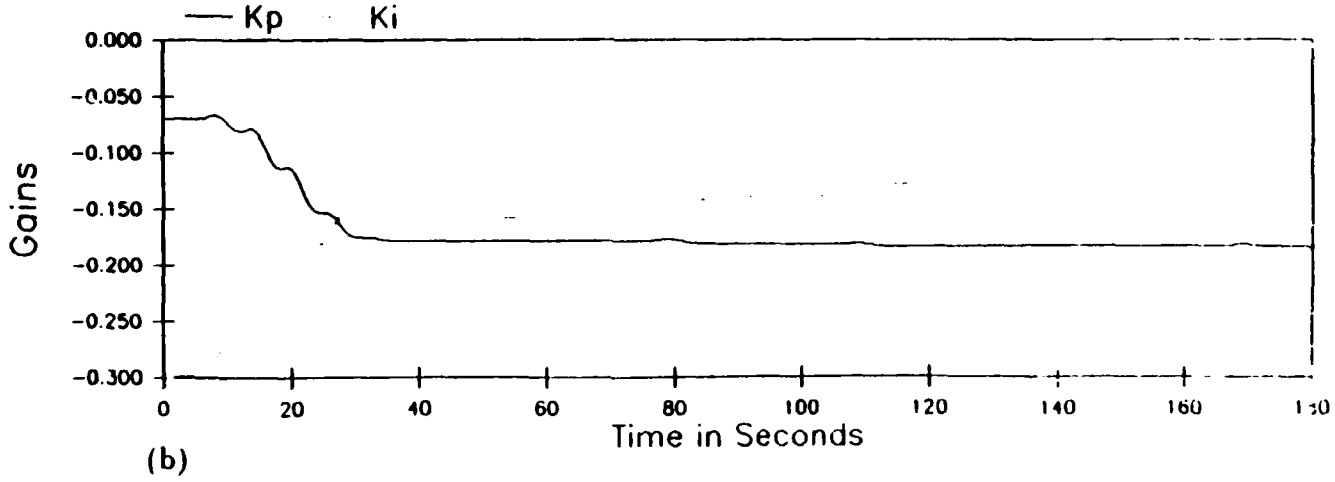

Figure 5.3 Results of simulation with operating point at 390 A, 1" thick plate. (a) Width response. (b) Parameter Convergence.

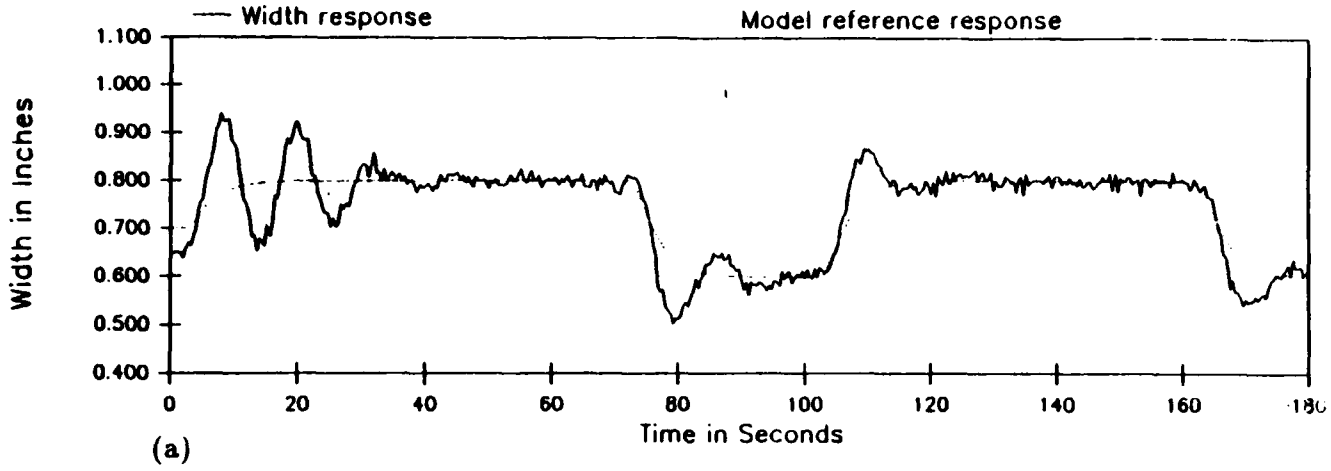

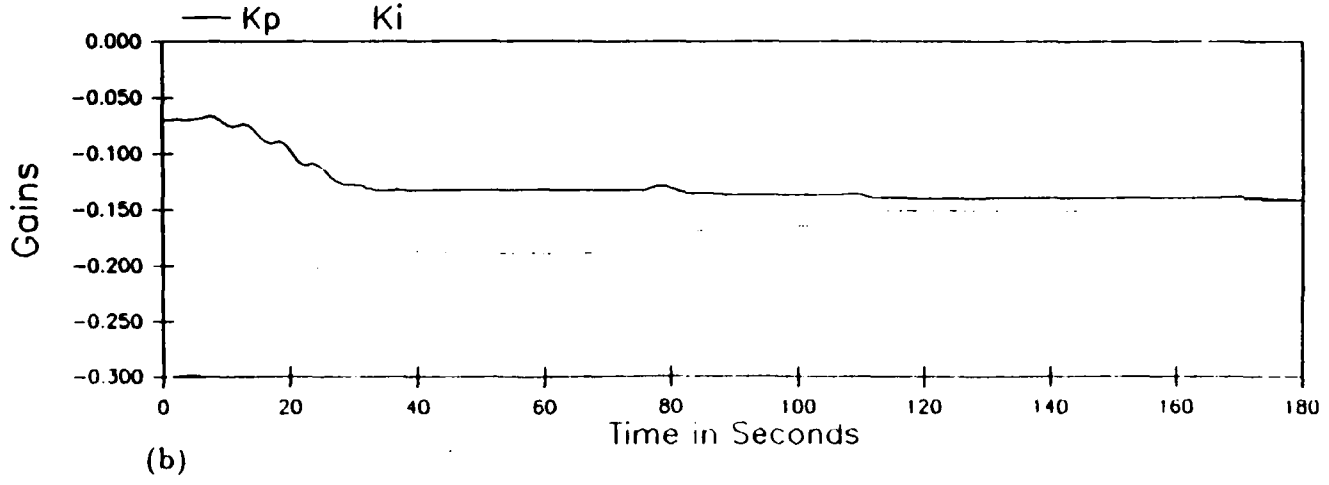

Figure 5.4 Results of simulation with operating point at 330 A, 1" thick plate. (a) Width response. (b) Parameter Convergence.

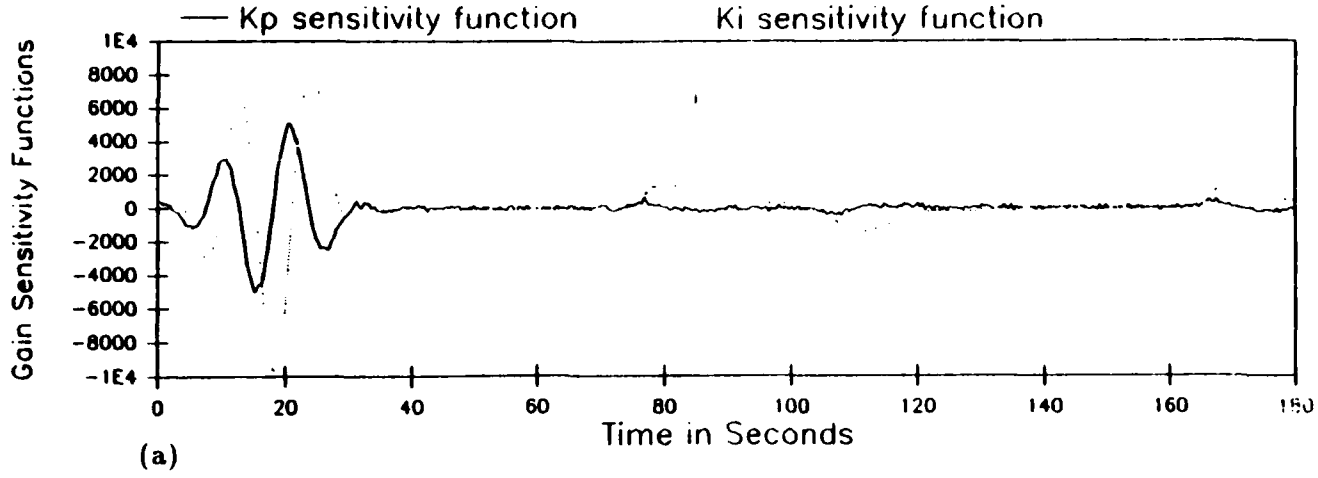

(a)

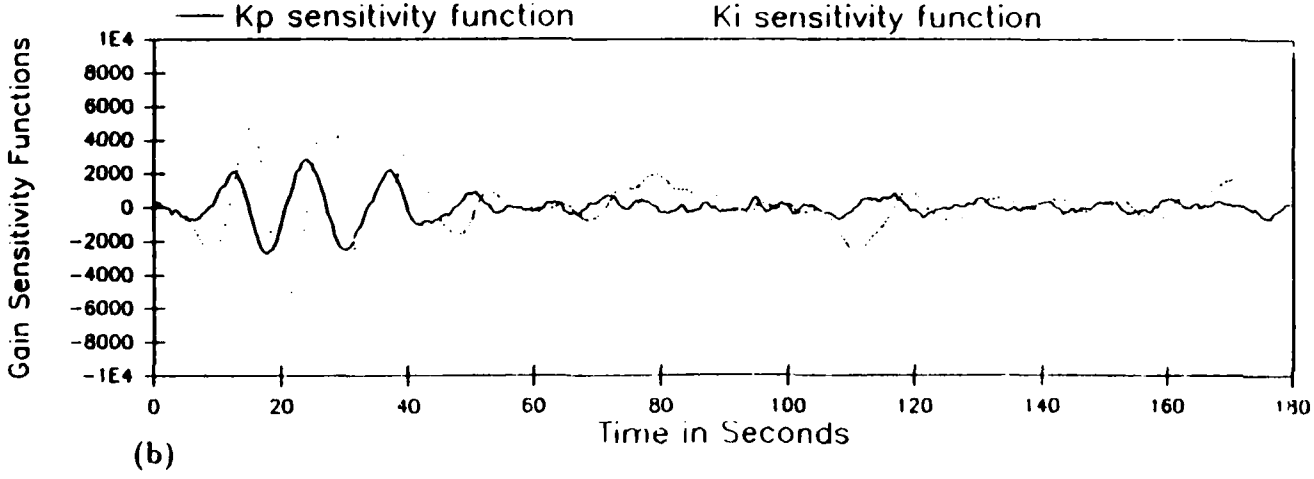

(b)

Figure 5.5 (a) Sensitivity functions for simulation at operating point with 360 A, 1" thick plate. (b) Sensitivity functions for experiment at operating point with 360 A, 1" thick plate.

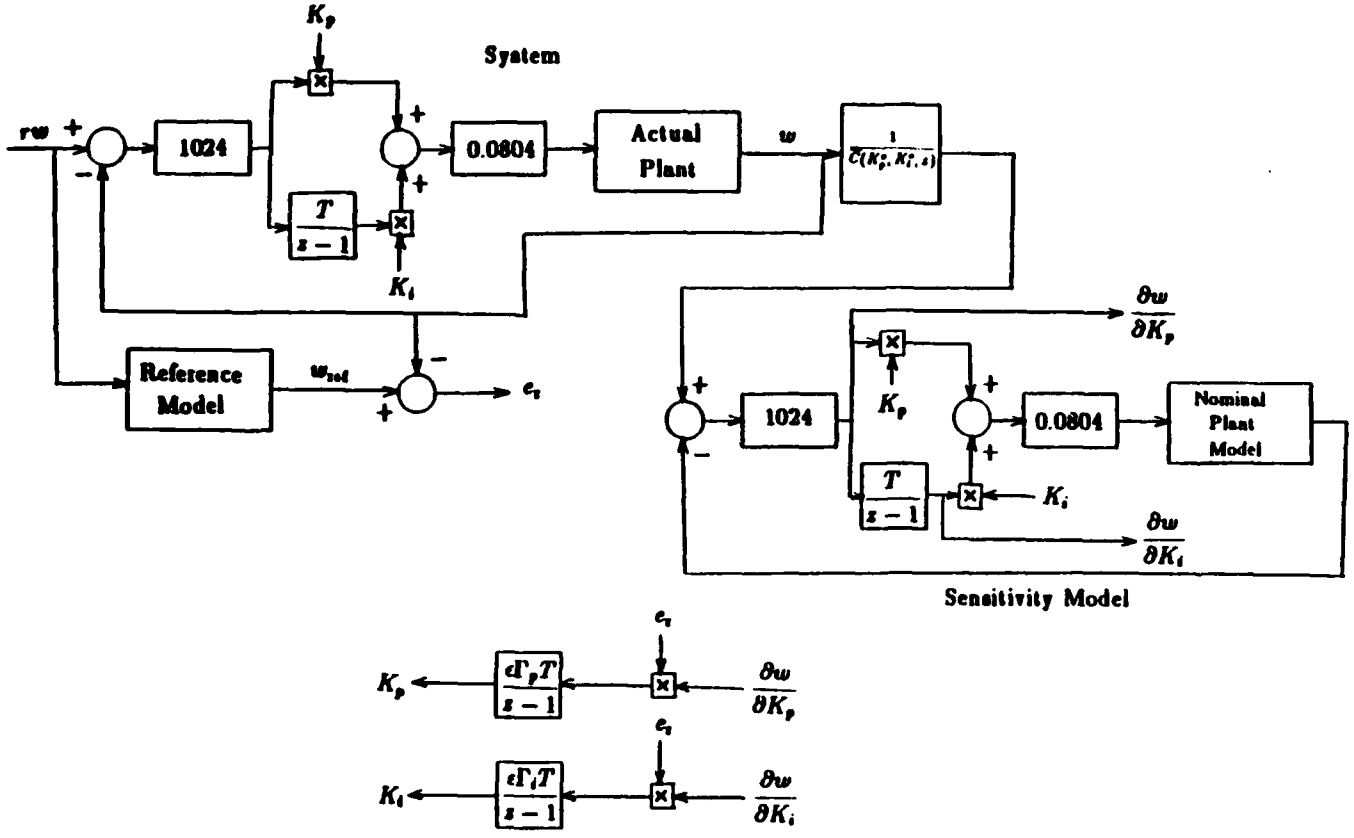

Figure 5.6 Block diagram of implemented adaptive control system.

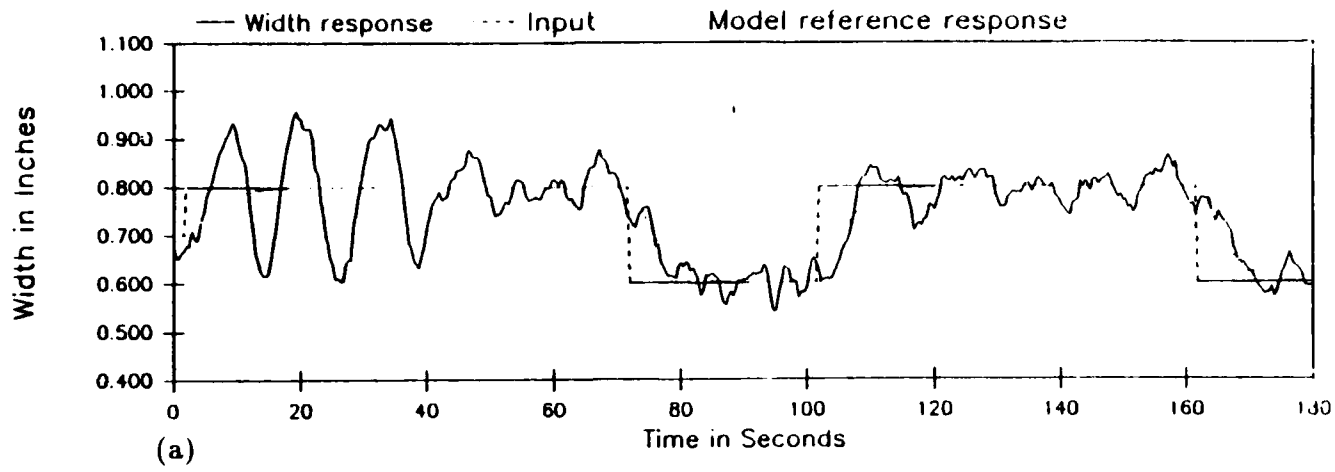

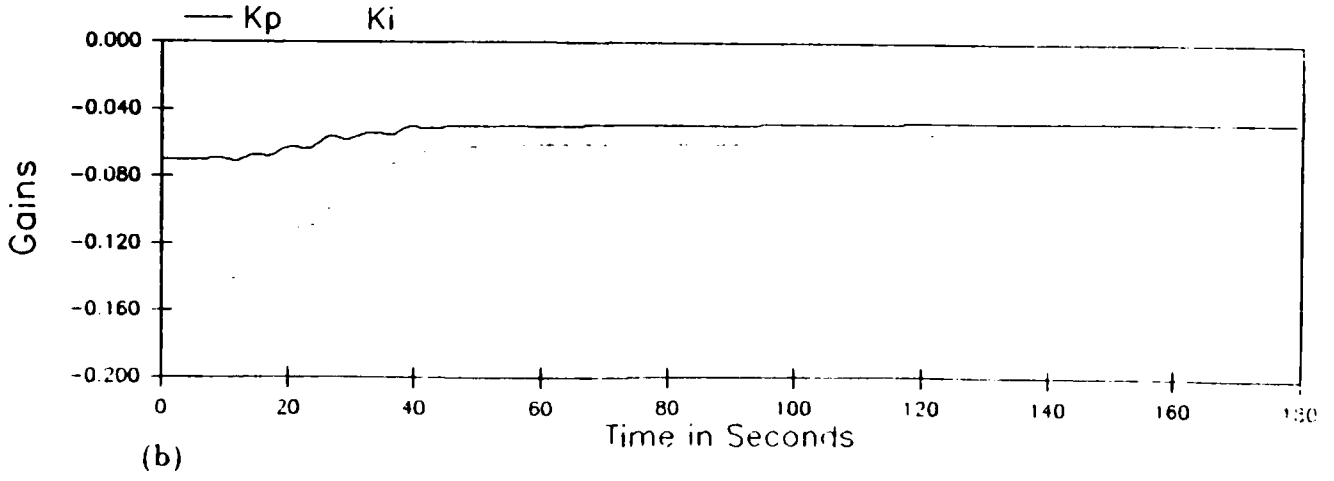

Figure 5.7 Results of experiment with operating point at 360 A, 1" thick plate. (a) Width response. (b) Parameter Convergence.

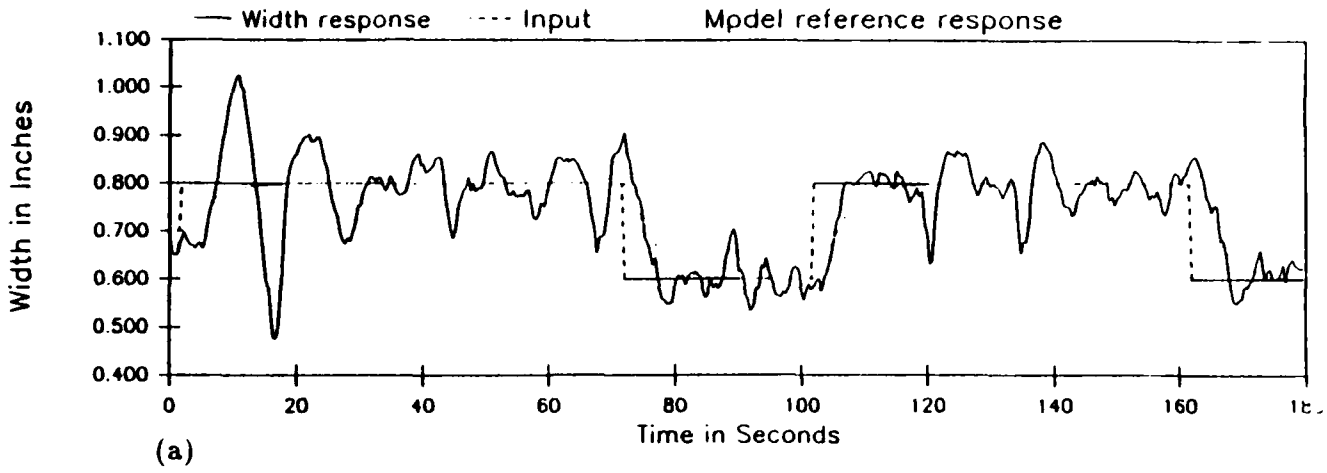

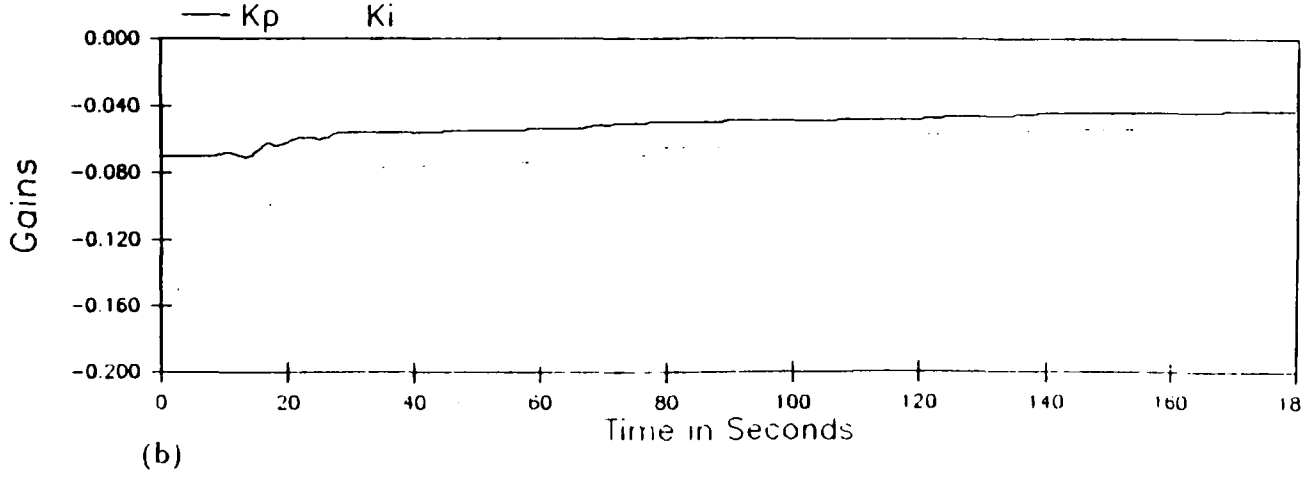

Figure 5.8 Results of experiment with operating point at 330 A, 1" thick plate. (a) Width response. (b) Parameter Convergence.

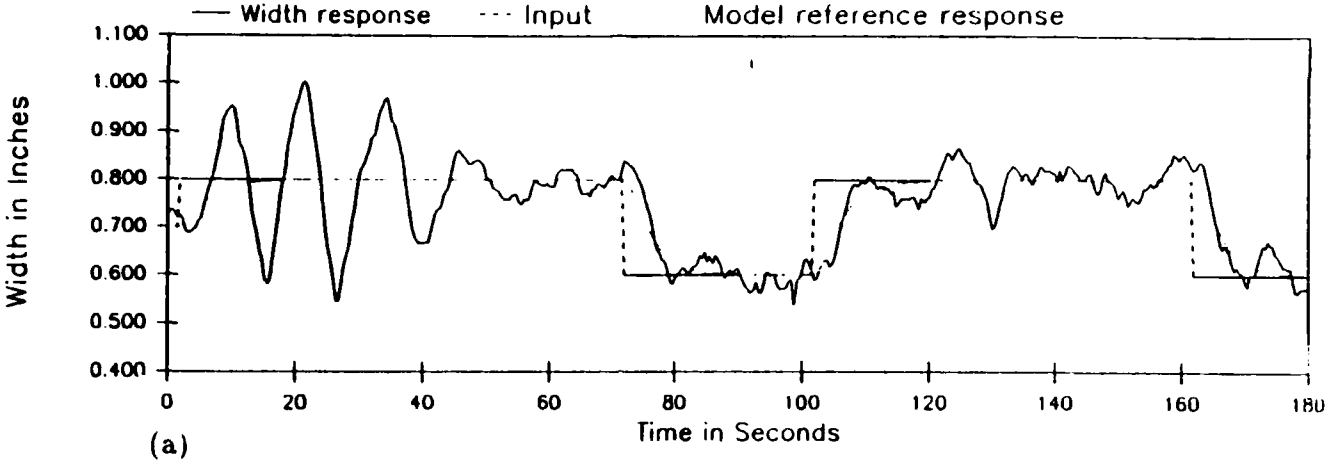

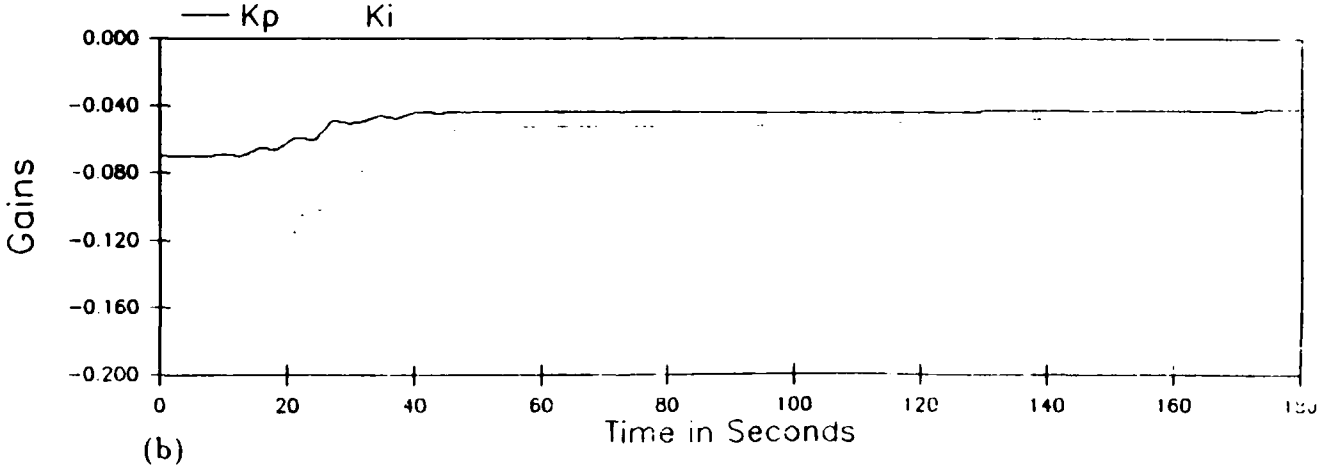

Figure 5.9 Results of experiment with operating point at 390 A, 1" thick plate. (a) Width response. (b) Parameter Convergence.

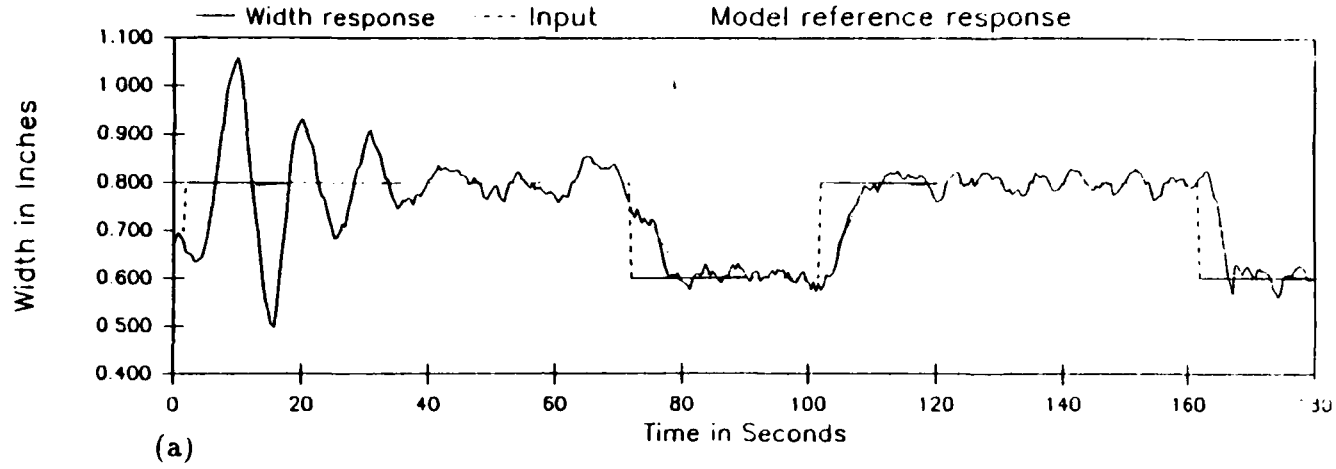

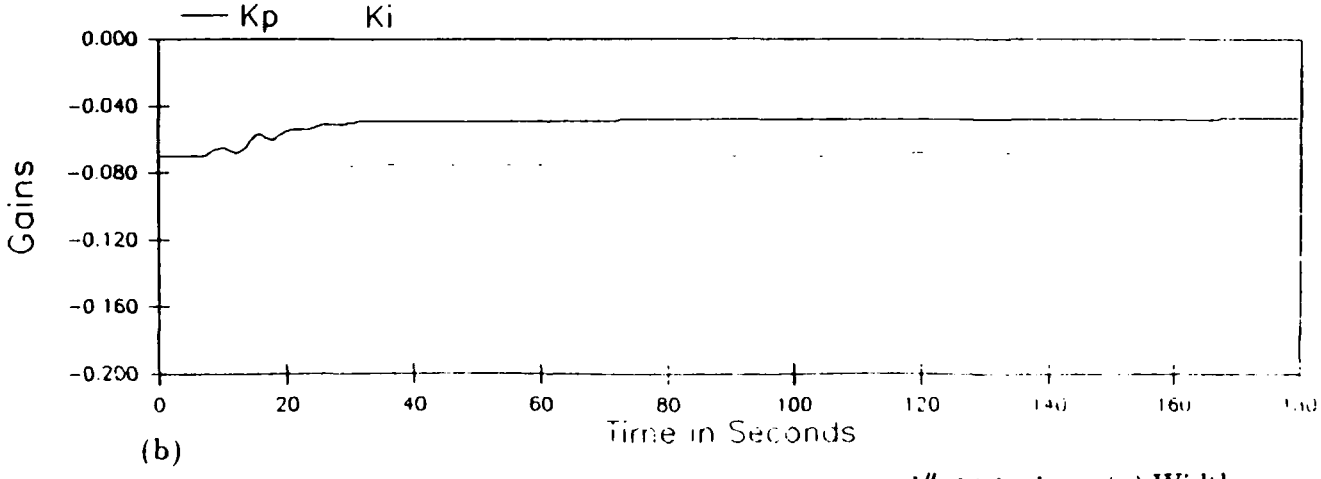

Figure 5.10 Results of experiment with operating point at 360 A, $\frac{1}{2}''$ thick plate. (a) Width response. (b) Parameter Convergence.

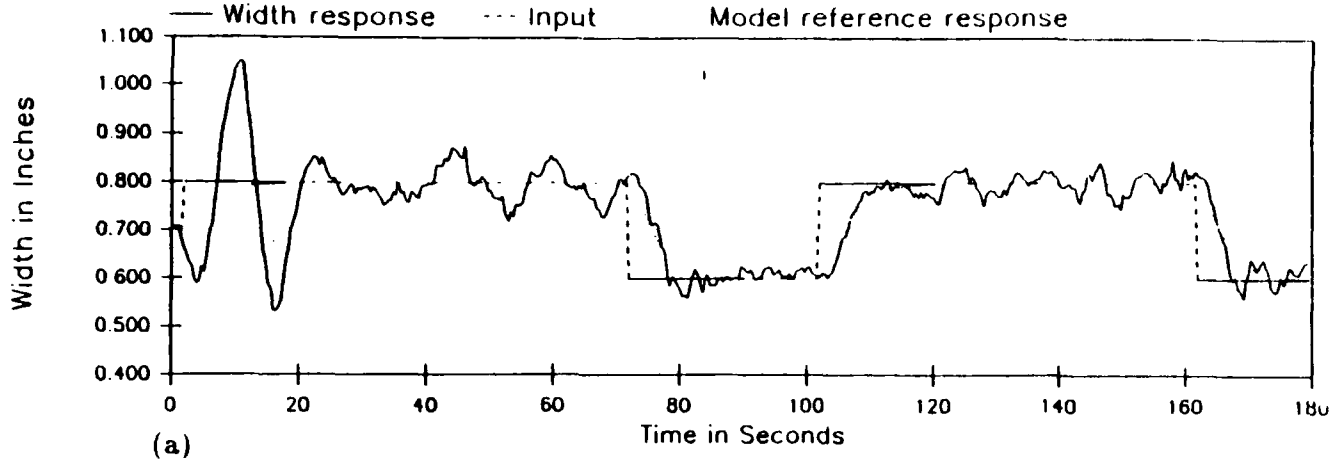

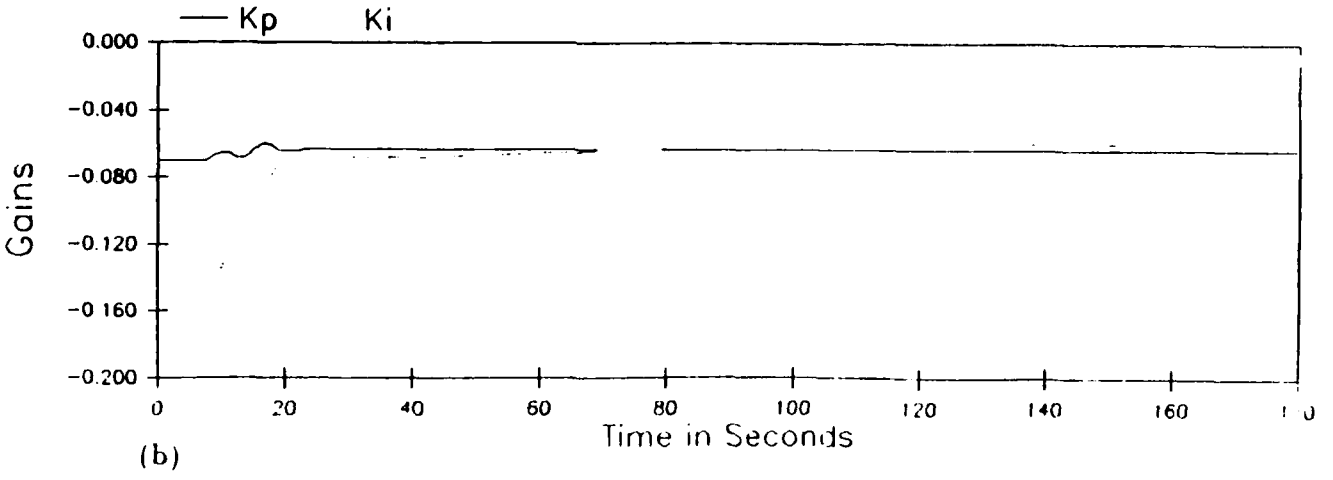

Figure 5.11 Results of experiment with operating point at 330 A, $\frac{1}{2}''$ thick plate. (a) Width response. (b) Parameter Convergence.

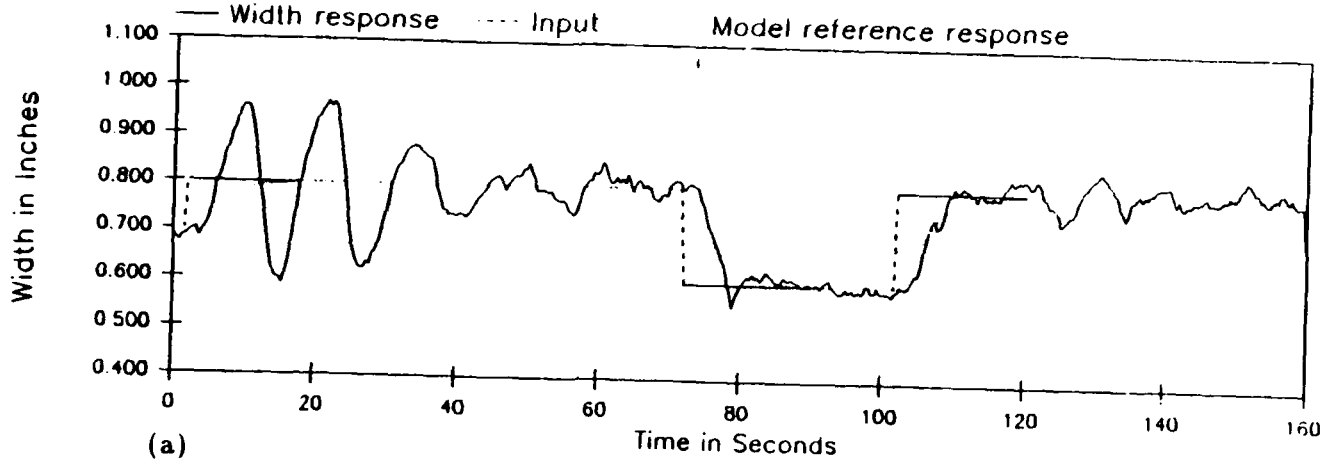

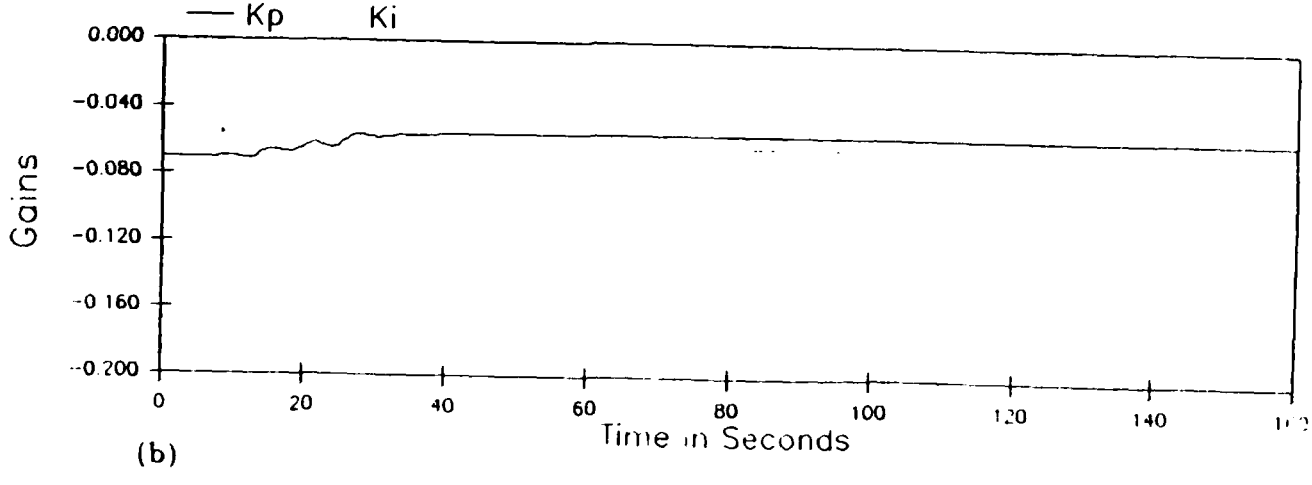

Figure 5.12 Results of experiment with operating point at 390 A, $\frac{1}{2}$" thick plate. (a) Width response. (b) Parameter Convergence.

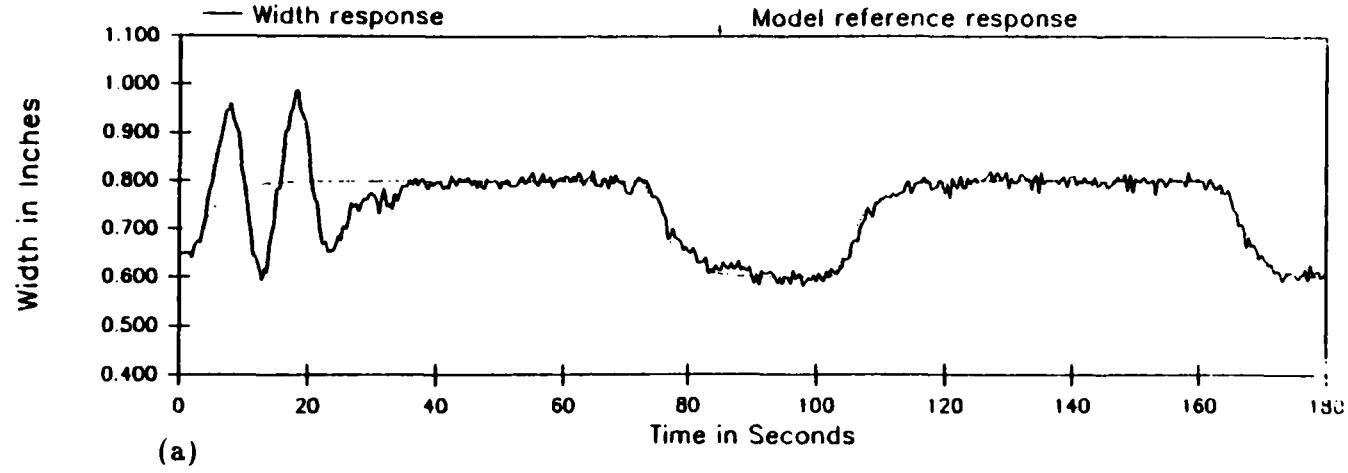

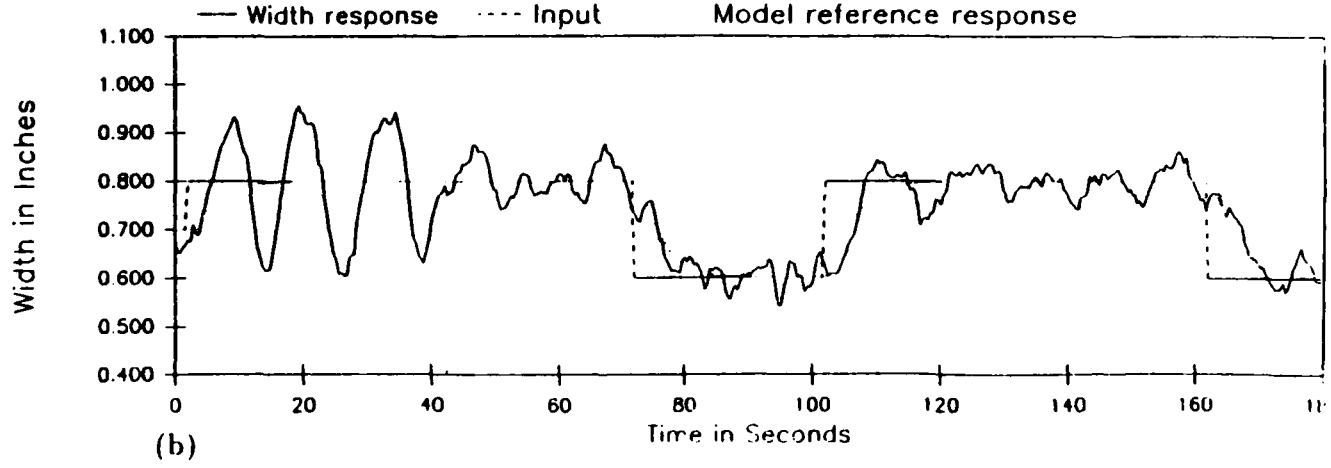

Figure 5.13 Comparison between simulated and experimental results for operating point at 360 A. 1" thick plate (a) Simulated results (b) Experimental results.

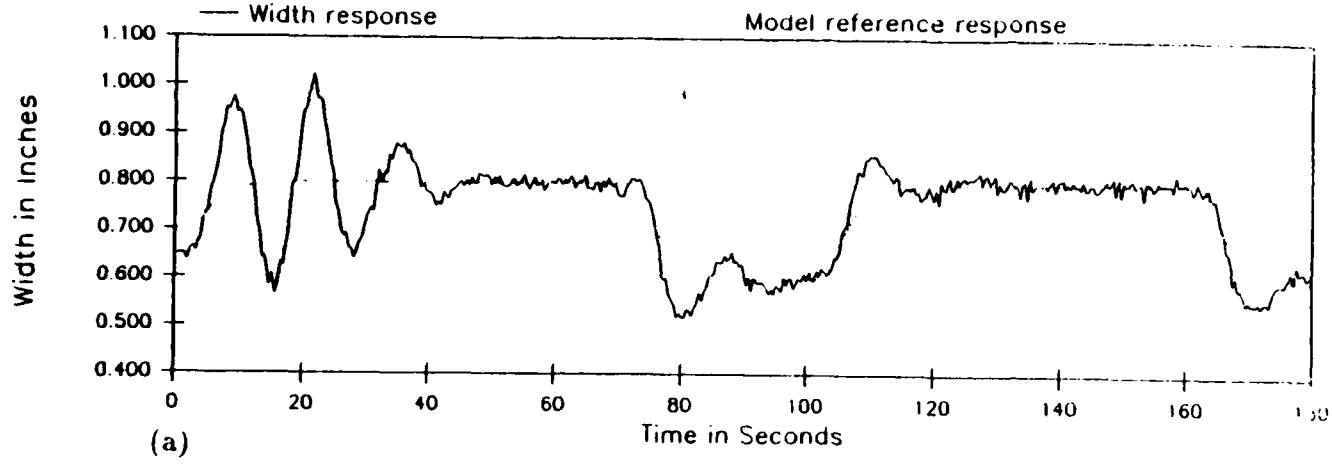

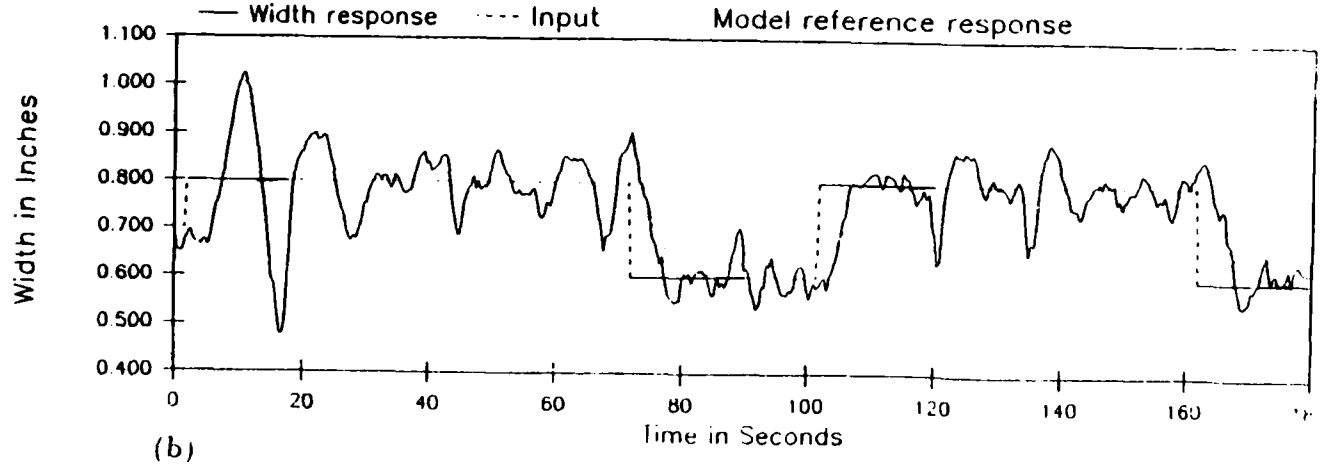

Figure 5.14 Comparison between simulated and experimental results for operating point at 330 A, 1" thick plate. (a) Simulated results. (b) Experimental results.

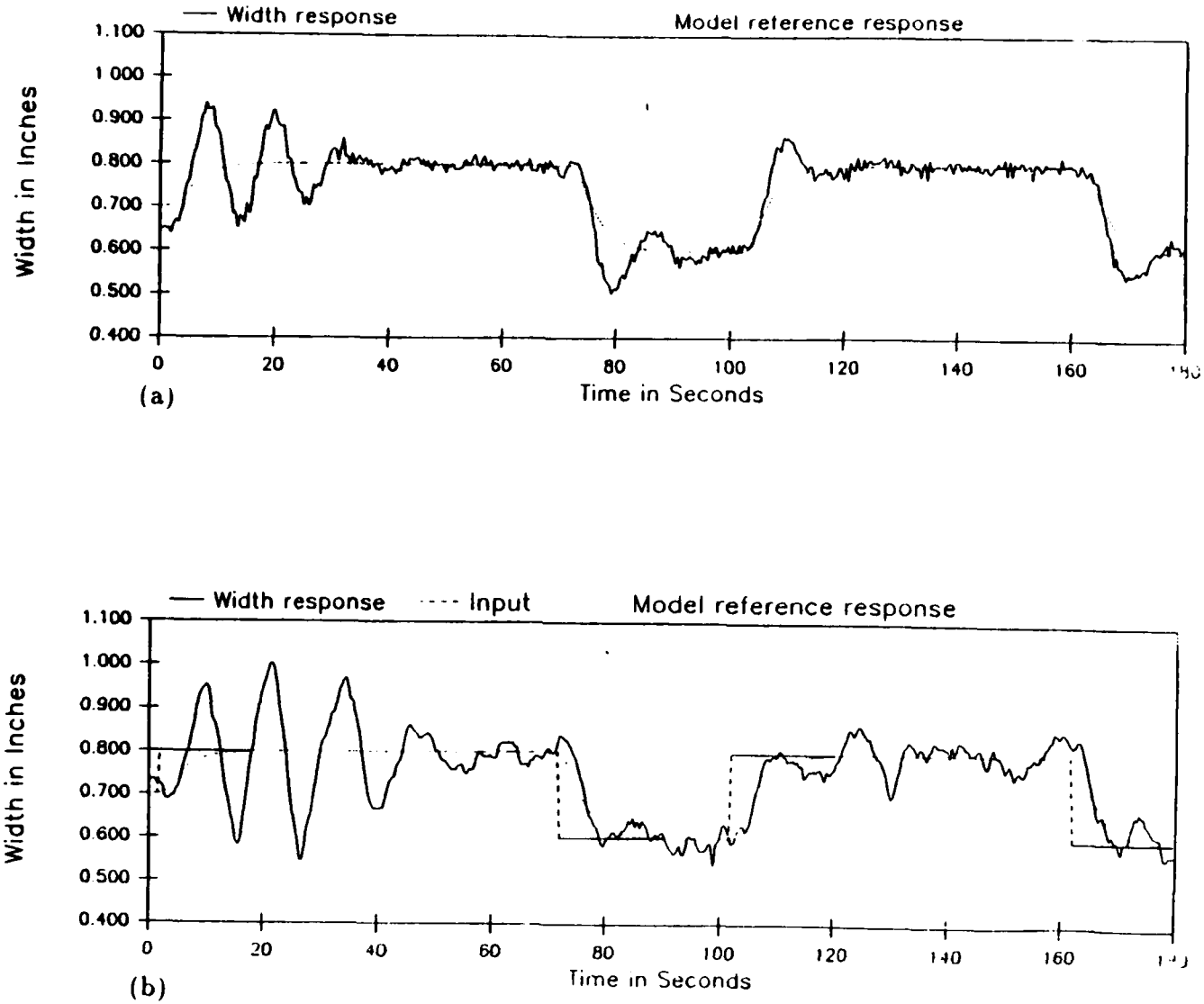

Figure 5.15 Comparison between simulated and experimental results for operating point at 390 A, 1" thick plate. (a) Simulated results. (b) Experimental results.

CHAPTER 6

CONCLUSIONS AND RECOMMENDATIONS

The method of sensitivity points has been developed for a weld puddle width control system incorporating a proportional plus sum controller. Sensitivity guided design and automatic tuning using both off-line and on-line methods have been presented for the weld puddle width system.

It was concluded that off-line tuning methods in general were not well-suited to the welding system because of its wide operating range. The welding control system has to be retuned whenever the operating point changes. The use of off-line tuning to accomplish this would be cumbersome and time-consuming. Therefore, these methods would be impractical.

However, the need for frequent retuning is a good reason for using on-line automatic tuning. As a result, an on-line adaptive system for controlling weld puddle width that performed well in simulation and experimentally was developed. The experimental results showed that the system could tune itself in a short amount of time. In view of this result, the best use of this system would be to use it to tune the weld puddle width controller whenever the operating point changes. These operating point changes correspond to things such as changing the type or thickness of the workpiece, or changing the shield

gas composition. In general, it is known when an operating point changes. Therefore, one possible method of using this system would be to perform a short tuning weld after on operating point change, and then use the resultant tuned controller as a fixed gain controller for the rest of the operation at this operating point.

An interesting possibility for the welding system would be to extend the results presented here by developing a multiple-input multiple-output (MIMO) sensitivity-method-based direct adaptive control system for controlling puddle width and area simultaneously. Torch travel rate could be used, as it is here, to control puddle width, and arc current could be used to control puddle area. This type of system would be an extension of the MIMO sensitivity method results presented by Hung [21].

Based on the experimental results, the direct adaptive puddle width control system presented here is successful in tuning the system to achieve the desired response over a wide range of operating conditions.

APPENDIX

EXPERIMENTAL SETUP

Gas Cup Height: $\frac{5}{8}''$

Preheat Plate Surface Temperature: 250°

Shield Gas Composition: 92%Ar, 8%CO_2

Shield Gas Flow Rate: 35 CFM

Linde Power Supply Type SVI-600 Settings:
slope: 1
inductance: $5\frac{1}{2}$
voltage: $7\frac{1}{2}$

Sony CCD XC-57 Video Camera Lens Settings:
Cosmicar 12.5 mm Television Lens:
focus: 0.3 m
fstop: 11
Sellstrom Shade 7 Gold Plated Lens
Tiffen Red 1 Lens
Tiffen Haze 1 Lens

Image Processing System Settings:
number of search vectors: 22
search angle: 10° to 100°
pixel y-position of electrode center: 515

REFERENCES

[1] N. D. Malmuth, W. F. Hall, B. I. Davis, and C. D. Rosen, "Transient thermal phenomena and weld geometry in GTAW," *Welding Journal*, Research Supplement., vol. 53, no. 9, pp. 388s-400s, 1974.

[2] A. R. Vroman and H. Brandt, "Feedback control of GTA welding using puddle width measurements," *Welding Journal*, vol. 55, no. 9, pp. 742-749, 1976.

[3] R. W. Richardson, D. A. Gutow and S. H. Rao, "A vision based system for arc weld pool size control," *Proceedings of the Conference of the American Society of Mechanical Engineers*, New York, pp. 65-75, 1982.

[4] R. W. Richardson, D. A. Gutow, R. A. Anderson, and D. F. Farson, "Coaxial arc weld pool viewing for process monitoring and control," *Welding Journal*, vol. 63, no. 3, pp. 43-50, 1984.

[5] N. R. Corby, "Machine vision algorithms for vision guided robotic welding," *Proceedings of the 4th International Conference on Robot Vision and Sensory Controls*, London, pp. 137-147, 1984.

[6] R. S. Baheti, "Vision processing and control of robotic arc welding system," *Proceedings of the 2nd Conference on Decision and Control*, Ft. Lauderadale, FL, pp. 1022-1024, 1985.

[7] A. Suzuki and D. Hardt, "Application of adaptive control to in-process weld geometry control," *Proceedings of the 1987 American Control Conference*, Minneapolis, MN, pp. 723-728, 1987.

[8] K. J. Aström and B. Wittenmark, *Computer Controlled Systems, Theory and Design*. New Jersey: Prentice-Hall, 1984.

[9] P. M. Frank, *Introduction to Sensitivity Theory*. New York: Academic Press, 1973.

[10] C. M. Adams, "Cooling rates and peak temperatures in fusion welding," *Welding Journal*, vol. 37, no. 5, Research Supplement., pp. 210s-215s, 1958.